PEDESTRIAN COLLISION RESPONSES USING LEGFORM IMPACTOR SUBSYSTEM AND FULL-SIZED PEDESTRIAN MODELS ON DIFFERENT WORKBENCHES

A Thesis by

Obaidur Rahman Mohammed

Bachelor of Technology, Jawaharlal Nehru Technological University, 2012

Submitted to the Department of Mechanical Engineering
and the faculty of the Graduate School of
Wichita State University
in partial fulfillment of
the requirements for the degree of
Master of Science

December 2016

PEDESTRIAN COLLISION RESPONSES USING LEGFORM IMPACTOR SUBSYSTEM AND FULL-SIZED PEDESTRIAN MODELS ON DIFFERENT WORKBENCHES

The following faculty members have examined the final copy of this thesis for form and content, and recommend that it be accepted in partial fulfillment of the requirement for the degree of Master of Science with a major in Mechanical Engineering.

_____
Hamid M. Lankarani, Committee Chair

_____
Rajeev Madhavannair, Committee Member

_____
Krishna Krishnan, Committee Member

DEDICATION

To My Parents, who kept me continuously motivated with their great support and encouragement throughout my MS program.

ACKNOWLEDGEMENTS

I would like to express my deep appreciation to my advisor, Dr. Hamid Lankarani whose understanding, guidance, patience and support have made it possible for me to work on an exciting topic. It was a great pleasure and honor working under guidance of his invaluable knowledge. He has always been kind and supportive when I look for help. I would again express my gratitude to him.

I would thank director and staff of the Computational Mechanics Laboratory in the National Institute for Aviation Research at Wichita State University for being so encouraging during my work in the laboratory and providing the huge opportunity with numerous computational resources for me to develop my engineering skills and to improve my knowledge. I would also convey special thanks to my friends, Salah, Viquar, Aamer, Ranjeeth, Gibran, Naveed, Imran, and all other friends for their valuable support when I need help.

Last but not least, I would deeply thank my parents, Dr. M.F. Rahman, and my brothers Habeeb and Sayeed for their endless support and encouragement.

ABSTRACT

Car-pedestrian collision fatalities have been reported for a significant number of roadside accidents around the world. Protection of pedestrians is taking on an increasingly significant role to car manufactures in developing new designs. The dynamic responses of the pedestrians in vehicle crashes can better be evaluated by examining the biomechanical responses. In order to reduce the lower extremity injuries in car-pedestrian collisions, it is important to determine the impact forces on the pedestrian and conditions that the car frontal side impacts on the lower extremities of the pedestrian. The Working Group 17 (WG17) of the European Enhanced Vehicle-safety Committee (EEVC) has developed a legform subsystem impactor and procedure for assessing pedestrian collisions and potential injuries. This study describes a methodology for the evaluation of the legform impactor kinematics after a collision utilizing finite element (FE) models of the legform and cars, and comparing the simulation results with the ones from a multi-body legform model as well as a 50th percentile male human pedestrian model responses. Two approaches are carried out in the process. First, the collision strike simulations with the FE model using an FE lower legform is considered and validated against the EVVC/WG17 regulation criteria. Secondly, the collision strike simulations with a multi-body legform and an ellipsoidal multi-body car model are conducted to compare the responses from the FE model and the multi-body model. The results from the impact simulations of FE legform and the multi-body legform are also compared with the ones from a full-size pedestrian model at different speeds. All the FE models of the legform impactor and the car model are developed and evaluated using the LS-DYNA nonlinear FE code, while the multibody legform, car, and full-sized pedestrian models are developed and evaluated in MADYMO. The results from this study demonstrate the differences between the subsystem legform and the full-size pedestrian responses as well as suitability of various FE and multibody models related to pedestrian impact responses.

TABLE OF CONTENTS

Chapter **Page**

TABLE OF CONTENTS (continued)

Chapter **Page**

LIST OF FIGURES

Figure **Page**

LIST OF FIGURES (continued)

Figure **Page**

LIST OF FIGURES (continued)

Figure **Page**

LIST OF FIGURES (continued)

Figure **Page**

LIST OF TABLES

Table **Page**

LIST OF ABRREVIATIONS

FARS	Fatality Analysis Reporting System
EEVC	European Experimental Vehicle Committee
HIPRC	Harborview Injury Prevention and Research Center TTI
TTI	Thorax Trauma Index
NCAC	National Crash Analysis Center ATD
ATD	Anthropomorphic Testing Device
FEM FEM	Finite Element Method
AIS	Abbreviated Injury Scale
GSI	Gadd Severity Index
HIC	Head Injury Criterion
NIC	Neck Injury Criterion
FMVSS	Federal Motor Vehicle Safety Standards
EEVC EEVC	European Passive Safety Network
NHTSA	National Highway Traffic Safety Association
FAA FAA	Federal Aviation Administration
FlexPLI	Flexible Pedestrian Legform Impactor

CHAPTER 1

INTRODUCTION

1.1 Background

Among all road user categories, pedestrians are the most vulnerable road users since they are unprotected in vehicle impact scenarios. Pedestrians are the second largest category of motor vehicle deaths after occupants. Each year thousands of pedestrians are killed or injured in road traffic accidents over the world resulting in substantial economic losses due to fatalities and long-term consequences. About 5,000 pedestrians are killed in motor vehicle accidents each year in the United States, and approximately 69,000 others are injured. This accounts for 13% of the nation's total traffic fatalities and 5% of injuries (FARS, NASS, GES). The proportion of pedestrian fatalities is a great concern in many other countries, such as the United Kingdom, Germany, and Japan [1].

According to the data available from the U.S. Department of Transportation's Fatality Analysis Reporting System, in the year 2002, 4,808 pedestrians were killed in traffic crashes, a decrease of 13 % from the 5,549 pedestrians killed in 1992. There were 71,000 pedestrians injured in traffic crashes in 2002. One- fourth of the children between 5 and 9 years old killed in traffic crashes in 2002 were pedestrians, and 6% of all youth under age 16 injured in traffic crashes were pedestrians [2].

Studies have shown that as the impact speed decreases from the 40km/h to 30 km/h, the probability of severe head injury will decrease from 50% to lower than 25%. The number of the killed pedestrian is between 12-45 % while number of collision of pedestrian with vehicle represents 4-8% from the overall number of the traffic accidents. The result indicates to high risk of pedestrian death in Collision with vehicle. Majority of the collision ware occurred in urban

areas. Number of the killed pedestrians in urban areas was 68% from overall number of the killed pedestrians [2].

Pedestrians are primarily impacted by the vehicle front with a high frequency in vehicle-pedestrian accidents. Most of these impacts occur at crash speeds of up to 40kmph. Crash tests developed by government research laboratories and European Experimental Vehicle Committee (EEVC) are available for the data required. The subsystem test procedures can be implemented to detect the vehicle front local stiffness and impact energy which are the main factors to cause pedestrian injuries.

In order to develop a new vehicle with pedestrian friendly front that can meet the requirements of the system tests, it is necessary to have an effective approach for the new vehicle front design to minimize the risk of pedestrian injury in an unavoidable accident. Although the number of pedestrian deaths has decreased dramatically over the past two decades, they still account for 11 % of motor vehicle deaths.

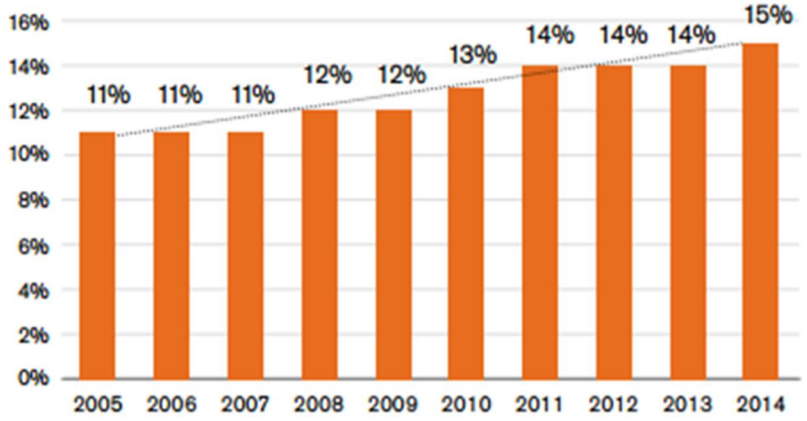

Figure 1.1 Pedestrian fatalities in US since 2005 [4].

As the number of Vehicle on the US highways continues to increase pedestrian fatalities also tends to increases. The pedestrian deaths as a percentage of total motor vehicle crash deaths increased steadily from 11 percent to 15 percent as shown in Figure 1.1. It has been 25 years (1990) since

pedestrians accounted for 15 percent of total traffic. With dramatically different size, shape, and stiffness than passenger cars, the LTVs may pose a more serious risk of injury and fatality for vulnerable road users such as pedestrians [2].

Pedestrian crash deaths comprise one part of the total deaths from motor vehicle crashes. From 1997 to 2006, there were 49,128 pedestrian fatalities, representing 12 percent all fatalities (424,840) in motor vehicle crashes. The rest of those killed in motor vehicle crashes were vehicle occupants (drivers and passengers), motorcycle riders, bicyclists, and others. Comparing the pedestrian fatalities by gender, female pedestrian fatalities account for 11 percent of the total females killed in motor vehicle crashes. Male pedestrian fatalities make up approximately 12 percent of the total males killed in crashes. Distribution of total motor vehicle in crash fatalities is shown in Figure 1.2 [3].

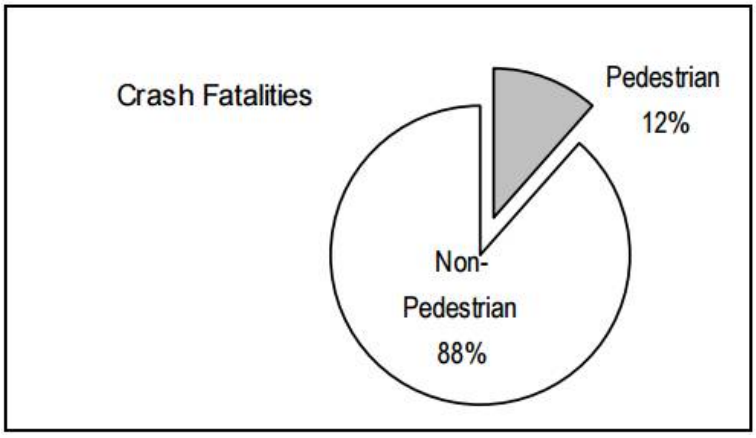

Figure 1.2 Distribution of total motor vehicle crash fatalities by person [3].

The number of deaths in motor vehicle crashes maintained at around 43,000 per year between 1997 and 2006. In some groups, notably among motorcycle riders, deaths have been increasing. Meanwhile, the pedestrian crash fatality rate continues a long-term decline. Since 1997, pedestrian fatalities have declined by 10 percent. This is the largest decrease in motor vehicle deaths among any person category.

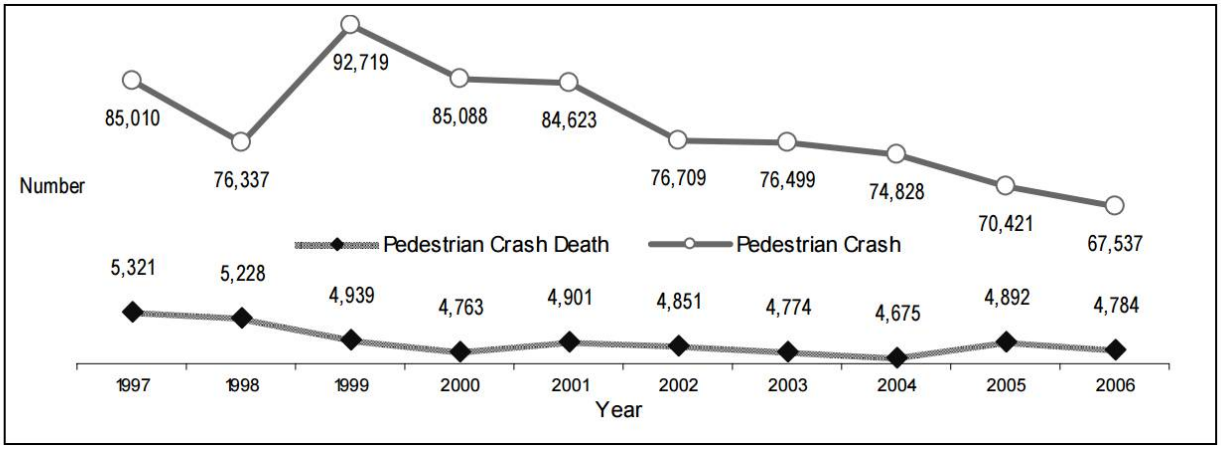

Figure 1.3 Pedestrian fatalities and reported pedestrian crasher by year [3].

A review of FARS data shows that pedestrian crash deaths declined between 1997 and 2006. In 1997, there were an estimated 85,010 police-reported pedestrian crashes, and 5,321 of those incidents resulted in pedestrian deaths. In 2006, these figures declined to 67,573 for total pedestrian crashes and 4,784 for pedestrian crash deaths, a 20-percent decrease for pedestrian crashes (subject to sampling errors) and 10-percent reduction for pedestrian crash deaths. This trend points out that pedestrian crashes are dropping faster than pedestrian crash deaths. Figure 1.3 shows pedestrian crashes on a downward trend since 1999 [3].

Pedestrians struck by light trucks had a three times higher risk of severe injuries and a 3.4 times higher risk of death, compared with pedestrians struck by passenger vehicles. The research was conducted by investigators based at the Harborview Injury Prevention & Research Center (HIPRC) and the Center for Applied Biomechanics at the University of Virginia. The evidence of a significantly greater risk of severe injury and death to pedestrians caused by light truck crashes supports the importance of technical tests to evaluate vehicle safety not only for passengers but also for pedestrians [4].

One study showed that about 85 % of pedestrian collisions occur in urban areas and about 15 percent in rural areas. However, 25 % of fatal pedestrian crashes occur in rural areas, reflecting

the generally more severe character of pedestrian collisions outside urban areas. Though most pedestrian crashes occur in urban areas, 60 % of all pedestrian crashes in urban areas do not occur at intersections. This compares to 75 % of child pedestrian crashes which occur not at an intersection. The percentages that do occur at intersections varies by crash type. Age is also a variable of importance, with 75 % of child pedestrian crashes not at intersections, contrasting with the majority of the elderly that do occur at intersections.

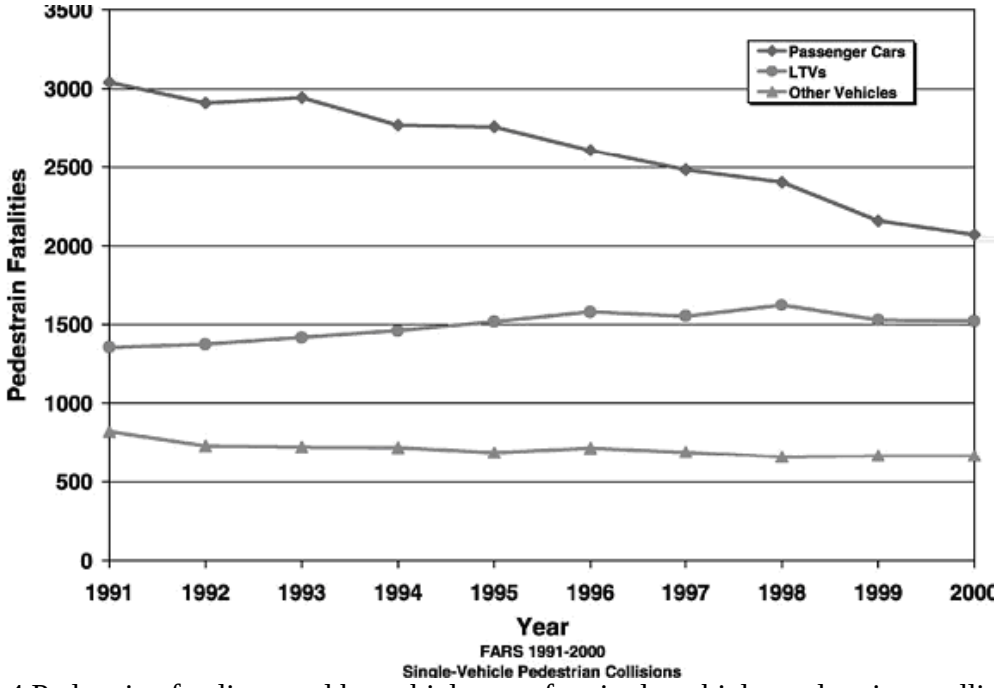

Figure 1.4 Pedestrian fatality trend by vehicle type for single vehicle–pedestrian collisions [5].

In 2000, 4739 pedestrians were fatally injured—an 18% decrease from 1991. In Figure 1.3 shows the overall trend in pedestrian fatalities from 1991 to 2000 [5]. When separated by vehicle type and restricted to single vehicle collisions. Although pedestrian fatalities resulting from car impacts decreased by 32% from 1991 to 2000, the number of pedestrian fatalities resulting from LTV impacts actually increased by 10% from 1991 to 2000 [5].

In U.S. pedestrian crashes in the Pedestrian Crash Data Study (PCDS), injuries to the lower extremity are greater than injuries to any other body region [6]. Among serious pedestrian injuries, lower extremity injuries are second in frequency only to head injuries. Approximately 80% of the

vehicle impact injuries to the thigh, knee, and lower leg are caused by bumper contact. Overall, 74 % of pedestrian crashes occur where there is no traffic control, 7 % where there is a stop sign, and 17 % in the presence of a traffic signal. Percentage variations in pedestrian crash are shown in Table 1.1 [6]. However, this breakdown greatly varies by crash type. When pedestrian crashes involve a vehicle turning at an intersection, 63 % occur where there is a traffic light, versus 17 % overall. With respect to speed limits, most pedestrian crashes occur where speed limits are low or moderate [7].

Table 1.1 Percentage of pedestrian crash types [8].

Pedestrian crash types	**% of crashes**
Crossing at intersection	32%
Crossing mid-block	26%
Not in road (e.g., parking lot, near curb)	9%
Walking along road/crossing expressway	8%
Backing vehicle	7%
Working or playing in road	3%
Other	16%
Total	**100%**

According to present statistics about police-reported motor vehicle crashes over time. Trends for fatal crashes and fatalities generally are presented from 1975 (when FARS began operation) to 2014. Figure 1.5 shows that Fatal crashes decreased by 0.7 percent from 2013 to 2014, and the fatality rate declined to 1.08 fatalities per 100 million vehicle miles of travel in 2014. The injury rate in 2014 remained at the 2013 level of 77 persons injured per 100 million vehicle miles of travel. The occupant injury rate (including motorcyclists) per 100,000 population, which declined by 13.6 percent from 1988 to 1992, decreased by 39.1 percent from 1992 to 2014 [6].

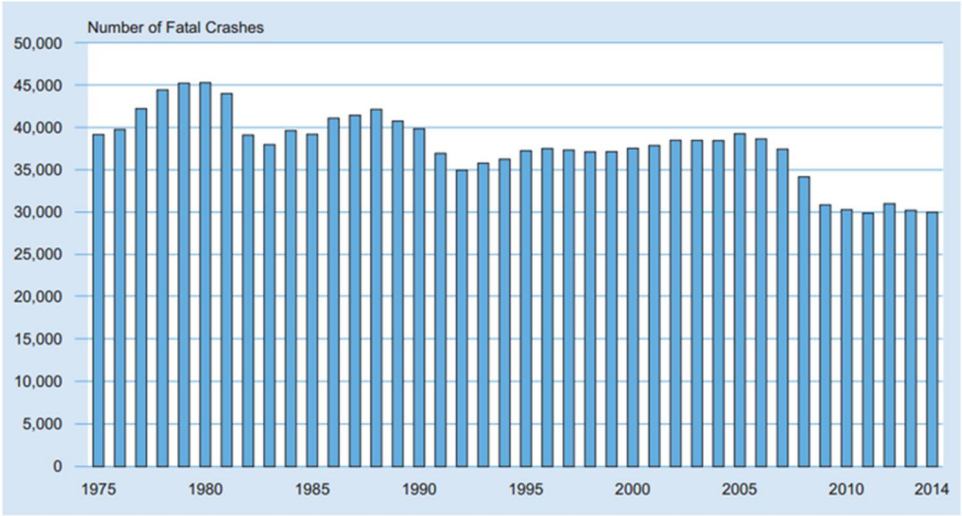

Figure 1.5 Proportion of vehicles involved in traffic crashes (FARS and GES, 1995–2015 [4].

The largest percentage of pedestrian fatalities falls into the 25-44 age category. However, when fatalities per 100,000 populations are calculated, the oldest age category stands out higher than the rest. Nevertheless, compared with their proportion in the U.S. population, children and young adults ages 2-22 are overrepresented in terms of pedestrian deaths and injuries. More male than female fatalities are seen in every age category. Even in the youngest age group, pedestrians less than 5 years of age, the population pedestrian death rate for males is 1.7 times greater than females, and males outnumber females in pedestrian collisions at the age of 2. Alcohol is an important factor in pedestrian crashes. Study showed that between 42 and 61 percent of fatally-injured pedestrians had BAC levels of 0.10 or greater. There is some indication that pedestrians who have been drinking pose a greater threat to pedestrian safety [4].

Figure 1.6 shows that all categories of passenger car have a higher pedestrian risk than light truck. When struck by a large van; 13.3% of pedestrians died as a result of the collision. In contrast, only 4.5% of pedestrian accidents involving a car resulted in a Pedestrian death. For large SUVs, 11.5% of pedestrian accidents resulted in a pedestrian fatality. We conclude that, a pedestrian struck by a van is nearly three times more likely to suffer fatal injury than a pedestrian

struck by a car. Pedestrians struck by large SUVs are twice as likely to die as pedestrians struck by cars [5].

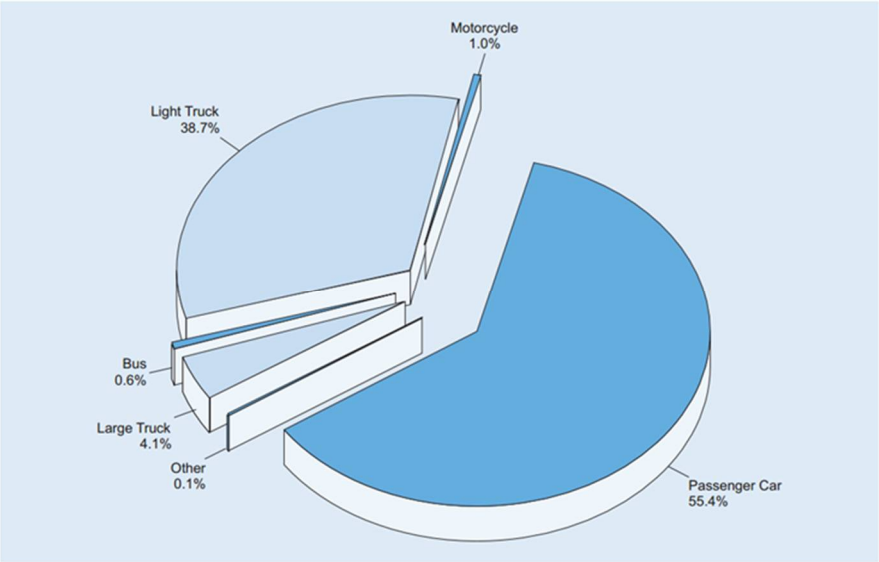

Figure 1.6 Pedestrian fatal crashes (FARS and GES, 1975-2014) [5].

Reducing pedestrian fatalities and serious injuries is a major concern in crash safety research. Recent accident statistics indicate that pedestrian fatalities account for almost 10% of all traffic related fatalities in Europe, 13% in the U.S, and almost 30% in Japan, among the advanced, industrialized nations [9]. The fraction of pedestrian fatalities and serious injuries are significantly higher in less developed countries where there has been a constantly increasing vehicle population [10].

In terms of the biomechanical responses, the injuries to the pedestrian are occurred in various parts of the body, but mostly in the primary impact of the leg region or the secondary impact of the head to the car windshield or pillars, or road surface. The Biomechanical limits for pedestrian impact tests are shown in Table 1.2 [1]. The limit for head injury is the same as Head Injury Criterion level for head impact inside a vehicle at the 15 percent confidence limits that a skull fracture is likely.

Table 1.2 Biomechanical limits for assessment of pedestrian impact tests [1].

Type of test	Injury Measurement	Units	Biomechanical Limits
Leg Form	Upper Tibia acceleration	g	<150
	Knee shear displacement	mm	<6
	Knee bending angle	degree	<15
Upper Leg Form	Bending Moment	Nm	<220
	Sum of force	kN	<4
Child Head Form	Head acceleration	HIC	<1000
Adult Head Form	Head acceleration	HIC	<1000

1.2 Motivation

Over the past few years, most attempts to reduce pedestrian fatalities and injuries have focused solely on isolation techniques, such as pedestrian bridges, public education, and traffic regulations [11-14]. Developing pedestrian-friendly vehicles is one solution for reducing the pedestrian fatality rate. Manufacturers currently attempt to produce enormous benefits for vehicle occupants enhancing pedestrian safety when impacting a vehicle with compliant bumpers, dynamically raised bonnets, and windscreen airbags [15-17].To assess the degree of pedestrian protection of a vehicle, it is necessary to develop an efficient evaluation and analysis methodology to examine vehicles for pedestrian protection. The EEVC, IHRA and Global Technical Regulation (GTR) have developed pedestrian subsystem test methods that assess vehicle capabilities to protect pedestrian during accidents.

In the late 1980s, the EEVC began developing a set of standards that can minimize serious injury to pedestrians when impacted by a vehicle traveling at 40 km/h [18]. The EEVC Working

Group 17 (WG17) established a series of component tests representing the three most important mechanisms of injury: head, upper leg, and lower leg. The EEVC WG17 proposed this method for assessing whether a vehicle was pedestrian friendly.

Recently, developments in computer technology have allowed applied mathematicians, engineers, and scientists to solve previously intractable problems. Simulation tools for predicting occupant or pedestrian kinematics and injury criteria include MADYMO, Pam Crash, and LS-DYNA3D [9].

To predict pedestrian injuries resulting from impacts with cars, full scale dummy, and pedestrian subsystem tests are used. In EEVC/WG17, the pedestrian protection test consists of three impact tests: the headform impactor to bonnet top test, the lower legform impactor to bumper test Pedestrian leg injuries because the leg is the most vulnerable body part in nonfatal pedestrian accidents (about 38% of all injuries) [19].

To consider and evaluate pedestrian fatalities, this study follows the WG17 regulations criteria for the pedestrian sub system models using computational methodoly. The kinematics of impactor subsystem to a car is quite evaluated for different workbenches in this study, In particular knee bending angle for the 50^{th} pedestrian model in contrast with FE impactor model. The main subject considered in legform impactor model is to achieve acceptable results by using particular test conditions in relatively less period of time. Consequently, there is a requirement to execute analysis by varying the parameters in simulations of FE legform model and multi-body model for proper investigation of the pedestrian injuries and pedestrian response with cars.

1.3 Literature Review

Teng, and Nguyen [20] presented a study on the development and validation of FE models of impactor for pedestrian testing. The certification of legform test was observed both static and dynamic impact simulations.

Paulozzi [21] described the relation between motor vehicle type and the risk of fatally injuring a pedestrian. The risk of killing a pedestrian was measured as the number of pedestrian fatalities per billion miles of vehicle travel by each vehicle type in the US in 2002 as reported by the National Highway Traffic Safety Administration's Fatality Analysis Reporting System. Rates for each vehicle type by sex, age, and rural/urban roadway type and rate comparisons using relative risks (RR) and 95% confidence intervals (CIs) are measured. Outcomes reflect the ways in which a vehicle's characteristics (mass, front end design, and visibility) and its degree of interaction with pedestrians affect its risk per mile. Modifications in vehicle design might reduce pedestrian injury. The greatest impact on overall US pedestrian mortality will result from reducing the risk from the light truck category.

Gabler and Hollowell [22] studied the aggressivity of light trucks and vans in traffic crashes. The goal of this paper is to examine LTV aggressively in vehicle-to-vehicle crashes. The specific objectives are to define the nature of the problem through examination of crash statistics, and to explore the relationships between crash aggressivity and vehicle design characteristics.

Abvabi Nasr study describes the Lower extremity injuries in vehicle-pedestrian collisions using a legform impactor model where the author has changed the material properties of the bumper [19].

Athale studied sensitivity analysis of pedestrian collision with a small car. This research concentrates on carrying out a sensitivity analysis for the pedestrian impact with small car and determines the injuries sustained by head from its resultant acceleration. The dummies used are 6-year-old child ATD, 5th percentile female Hybrid III ATD and 50th percentile male Hybrid III ATD at 3 different speeds [23].

Ronghe studied analysis of pedestrian-compact car, pedestrian-SUV impact. This research concentrates on the kinematic study of pedestrian-vehicle accident for 50th percentile male Hybrid III ATD, 6-year-old child ATD and 3-year-old child ATD with compact car, SUV and minivan.

Only side impact of the pedestrian with vehicle is considered at 2 different speeds [24].

Stammen research investigated the performance of the vehicle bumper system with EEVC Pedestrian Legform where it focused on the level of the pedestrian lower extremity protection offered by front bumper in the U.S [25].

Korrapati compared the kinematic responses of the Hybrid III standing dummy and pedestrian human model kinematics in vehicle-pedestrian collision [26]. This study was conducted to evaluate the effects of parameters such as bonnet height, bonnet angle, pedestrian impact positions and vehicle speed on the pedestrian impact responses.

1.4 Pedestrian Injury Criteria

Studies carried out since 1970's were based on different approaches with pedestrian substitutes such as biological specimens, mechanical dummies and mathematical models, as well as real world accident samples. Hence, injury levels, injury criteria, pedestrian injury biomechanics and its connection with the analysis of real-world car-pedestrian accident reconstruction are briefly described.

Injury biomechanics field deals with the effect of mechanical loads, in particular impact loads on the human body. Due to this mechanical load, a body region will experience mechanical or physiological changes. These changes are called the biomechanical responses. The mechanism involved is called the injury mechanism and the severity of the resulting injury is named as the injury severity. An injury criterion is a physical parameter or a function of several physical parameters, which correlates with the injury severity of the body region under consideration. There are many proposals for ranking and quantifying injuries. Anatomical scales describe the injury in terms of its anatomical location, the type of injury and its relative severity. The mostly accepted anatomical scale worldwide is the Abbreviated Injury Scale (AIS). The AIS distinguishes the following levels of injury in the Table 1.3

Table 1.3 Abbreviated Injury Scale (AIS) [27].

AIS Score	Injury
0	No injury
1	minor
2	moderate
3	Serious
4	severe
5	critical
6	Maximum injury
9	unknown

The numerical values have no significance other than to designate order. Many injury criteria are based on the acceleration forces, displacements, and velocities. Some injury criteria need mathematical evaluation of a time history signal. The biomedical codes including MADYMO offers the possibility to perform some of these injury parameter calculations.

An injury parameter is a physical parameter or a function of several physical parameters, which correlates well with the injury severity of the body region under consideration. Many schemes have been proposed for ranking and quantifying injuries.

Anatomical scales describe the injury in terms of its anatomical location, the type of injury and its relative severity. Most injury criteria are based on accelerations, relative velocities or displacements, or joint constraint forces. These qualities must be requested with standard output options. Most injury criteria need some mathematical evaluation of a time history signal. MADYMO performs these injury parameter calculations. The following injury parameter calculations are available [27].

* Gadd Severity Index (GSI)
* Head Injury Criterion (HIC)
* Neck Injury Criterion (FNIC)
* 3 ms Criterion (3MS)
* Thoracic Trauma Index (TTI)
* Femur Loads

Injury parameter calculations for the HIC, GSI and 3MS are carried out on the linear acceleration signal of a selected body. The TTI calculation is carried out on the linear acceleration signals of two selected bodies. These linear acceleration signals must have been defined under the LINACC keyword.

1.5 Pedestrian Injury Biomechanics

The most common pedestrian injuries include thorax to the lower and upper region as well as the head region of the body. This injury and their biomechanics evaluation are discussed here.

1.5.1 Head Injury Criterion

Head Injury Criteria (HIC) is frequently the most challenging standard to meet. J. Versace was the first to propose the Head Injury Criterion (HIC), and was later modified by NHTSA (8). This criterion is based on the interpretation of the Gadd Severity Index. HIC is an empirical formula based on experimental work. The HIC does not represent simply a maximum data value, but represents an integration of data over a varying time base. The HIC is based on data obtained from three mutually perpendicular accelerometers installed in the head of the ATD in accordance with the dummy specification. Head Injury Criterion (HIC) is developed as an indicator of the likelihood of severe head injury and is determined by [11]:

The Head Injury Criterion, or HIC, by NHTSA is described by the following expression [27].

$$HIC = \max_{t_1, t_2} \left\{ (t_2 - t_1) \left[\frac{1}{t_2 - t_1} \int_{t_1}^{t_2} a(t) dt \right]^{2.5} \right\}$$

Where:

t_1: Initial time (in s) of the interval during which HIC attains maximum value.

t_2: Final time (in s) of the interval during which HIC attains maximum value.

In automotive testing, HIC is calculated regardless of the presence of head contact. According to the Federal Motor Vehicle Safety Standards (FMVSS) and FAA regulations,the HIC should not exceed 1000 for 36ms Δt duration, or 700for 15 Δt duration.

1.5.2 Thorax

The lateral impact to the thorax is the most common in truck-pedestrian impact. The pedestrian thorax injury mechanism is typically associated with blunt trauma due to the flat bonnet top or the relative flat edge that impacting the thorax without penetration. The thorax contact location on the truck front is different due to the age and size of the pedestrians. The thorax injuries of adults and older children are mainly attributed to bonnet-top impacts. Small children are more likely to sustain thorax injuries at impact with the bonnet front edge and the end front face of the truck. In a truck-pedestrian lateral impact, the thorax is accelerated towards the bonnet and then decelerated suddenly due to a blunt bonnet impact. The thorax injuries can attribute to three mechanisms: the compression of the thorax, the viscous loading within the thorax cavity, and internal loading to the internal organs. A typical side view of the thorax structure shown in Figure 1.7.

The compressive force to the thorax can result in the rib fracture, sternum fracture, hemothorax, and pneumothorax. The thorax injuries in accident often take place in a combination with these three mechanisms. The thorax impact responses have been studied by many researchers using cadavers and volunteers. Some of the studies were carried out in a lateral

impact related to occupant side impact responses.

Results from such studies are valuable for study on biomechanical responses of pedestrian thorax to car front impact. The suggested tolerance level for TTI (Thoracic Trauma Index) for adult is 85g and for child 60g. The MADYMO analysis gives the Sternum Acceleration as output which can be used for TTI [23].

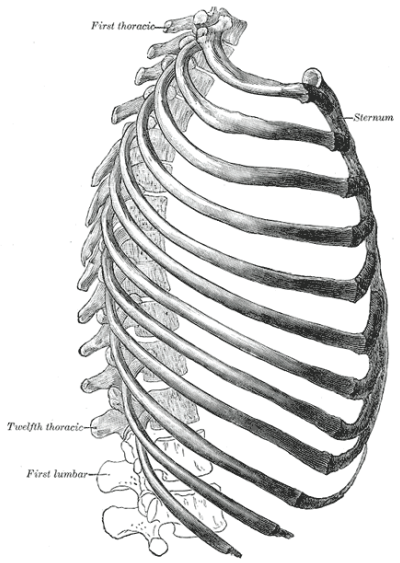

Figure 1.7 Side view of the thorax structure [28].

The suggested tolerance level for TTI (Thoracic Trauma Index) for adult is 85g and for chills is 60g. MADYMO analysis gives the sternum acceleration as output which can be used as TTI.

1.5.3 Pelvis

The pelvis shown in Figure 1.8 can be injured by lateral impact with a stiff bonnet edge or bonnet top. In Truck-Pedestrian impact, the compressive force to the pelvis is the dominated injury mechanism. The pelvis shown in fig. can be injured by lateral impact with a stiff bonnet edge or bonnet top. The injuries to this body segment often involve one or more of the following structures: pubis, acetabulum (hip socket), spine, and proximal femur. Accidents involving small

children are less likely to produce pelvis fracture than do accidents with adults.

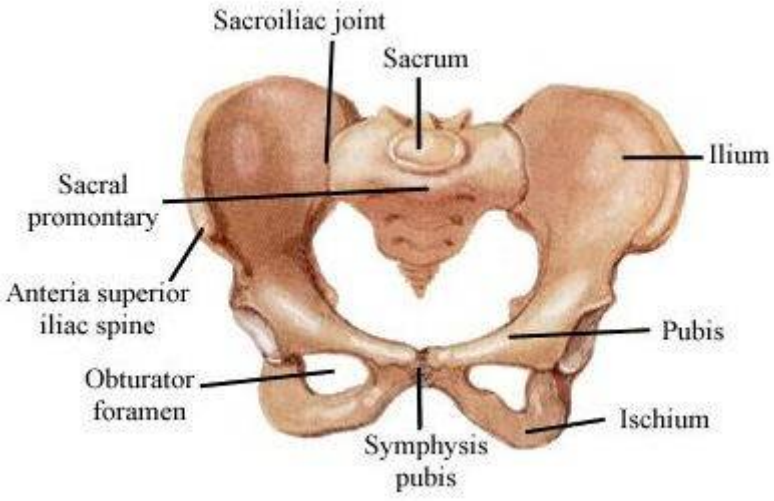

Figure 1.8 The body segments of pelvis [22].

The research on the responses of the pelvis to lateral impacts was conducted with cadaver specimens at different institutes. In these studies, the lateral responses have been described in terms of impact force time histories, acceleration time histories of the pelvis, and compressive deflection. The injury criterion for pelvis linear acceleration is 50g to 90g value [23].

1.5.4 Lower extremities

According to the EEVC working group responsible for the development of the impactor or as "TRL impactor" according to the company that had finalized the design and is merchandising the impactor now. It mainly consists of two stiff metal tubes, two deformable knee elements made of steel and a shearspring system with a hydraulic damper shown in Figure 1.9. The two stiff metal tubes represent the femur and the tibia of a human leg. The deformable knee elements represent the human knee, specifically the ligaments, with the ability to withstand a certain bending. The metal "ligaments" are used to assess possible knee injuries. The shear-spring system simulates lateral shear displacement between femur and tibia at the knee level; the damper is necessary to limit vibrations

caused by the mass of the shear-spring system. An accelerometer is used to indirectly measure the contact force applied to the tibia, representing a provisional assessment of the risk of bone fractures

Figure 1.9 FE legform model [29].

In car-pedestrian collisions fracture of the leg often occurs, especially of the lower leg. Therefore fracture joints have been implemented at the second upper leg joint and all three lower leg joints. All fracture joints are spherical joints. Initially, they are locked and will be unlocked as the local fracture trigger signal exceeds the fracture level. In the unlocked situation, there is no stiffness defined. A minor rotational damping has been defined to make the movement of the broken leg part realistic and avoid numerical instability problems. The fracture joints can also be switched off.

The leg is based on the physical pedestrian leg model that is comparable with the leg of the Hybrid III dummy model. In both the upper and lower leg spherical joints have been implemented in order to model bending and fracture [23]. Figure 1.10 show the schematic representation of major injuries and joints in a car-pedestrian lateral collision and MADYMO model. The following modes of injury to the lower extremity are most common in truck-pedestrian impact: long bone (Thigh bone/Femur and Legs/Fibula-Tibia) fractures, knee injuries, and ankle/foot dislocation and fracture.

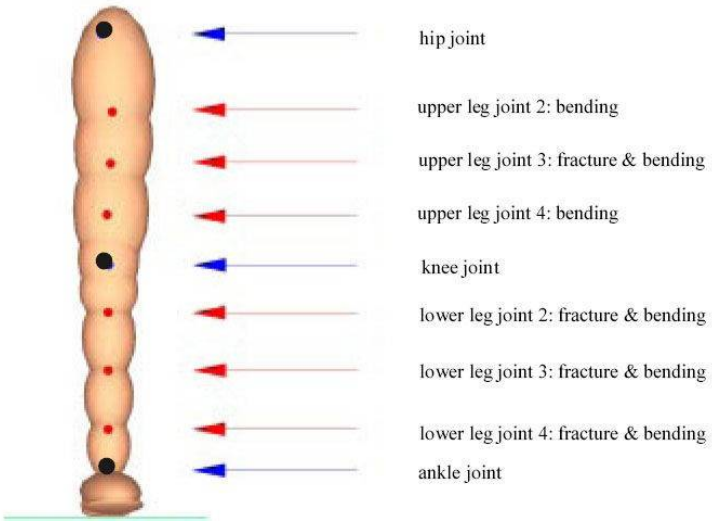

Figure 1.10 MADYMO pedestrian leg model [29].

The impact with the truck front and the subsequent acceleration of the pedestrian's lower extremities result in complex injury mechanisms. Lateral shearing and bending have been recognized as the two most important injury-related reactions of pedestrian lower extremities to a bumper impact.

1.6 EEVC Testing Method

In the European Union more than 7000 pedestrians and 2000 pedal cyclists are killed every year in a road accident, while several hundred thousands are injured. However, differences between the individual member countries are remarkable. Annual pedestrian fatalities per million inhabitants rank from 10 in the Netherlands to 47 in Greece. Pedestrian fatalities per 100 road accident fatalities rank from 12 in France to 32 in Great Britain [30]. A large proportion of pedestrians and cyclists are impacted by the front of a passenger car. This was recognized by the European Enhanced Vehicle safety Committee (the former European Experimental Vehicles Committee) and several studies in this field were performed by Working Groups of EEVC [31-35]. Based on this research various recommendations for the front structure design of passenger cars were developed. Moreover, test methods and regulations have been proposed to assess pedestrian protection. In the spring of 1987

one of these proposals was discussed by the EEC ad-hoc working group 'ERGA Safety' [36]. It was concluded that the basis of the proposal was promising, however, additional research was needed to fill up some gaps. The EEVC was asked to co-ordinate this research and at the end of 1987 EEVC Working Group 10 µPedestrian Protection was set-up.

The mandate of this group was to determine test methods and acceptance levels for assessing the protection afforded to pedestrians by the fronts of cars in an accident. The test methods should be based on sub-system tests, essentially to the bumper, bonnet leading edge and bonnet top surface. The bumper test should include the air dam; the bonnet leading edge test should include the headlight surround and the leading edge of the wings; the test to the bonnet top should include the scuttle, the lower edge of the windscreen frame and the top of the wings. Test methods should be considered that evaluate the performance of each part of the vehicle structure with respect to both child and adult pedestrians, at car to pedestrian impact speeds of 40 km/h. The different impact characteristics associated with changes in the general shape of the car front should be allowed for by variations in the test conditions (e.g. impact mass and velocity, direction of impact).

The EEVC WG10 started its activities in January 1988. Both governments (mostly represented by research institutes) and automobile industry were represented in the working group. A programme was set-up intended to develop the required test methods as described by the mandate. The studies necessary to develop test methods have been summarised in a first report of EEVC WG10, presented to the 12th ESV Conference in 1989 [37]. These development studies included full scale dummy tests, cadaver tests, accident reconstructions, analysis of accident data and computer simulations. Furthermore the developed test proposals had to be tested against representative cars of current designs to determine the feasibility of the proposals. The compatibility with existing regulations, other safety features and basic operational requirements for cars was assessed. These studies were performed in 1989/1990 by a European consortium acting under contract to the European

Commission and under the auspices of EEVC. The consortium consisted of BASt, INRETS, LAB/APR, TNO and TRL. The studies were completed in June 1991 and were summarised individually in technical reports [38-41]. The summary report [42] included an Annex called "Frontal surfaces in the event of impact with a vulnerable road user - proposal for test methods". This work was also summarised in a second EEVC WG10 report, presented to the 13th ESV Conference in 1991 [43].

The third and final report of EEVC WG10 was written in 1994 [44] and focused especially on the changes and improvements with respect to the previous version of the proposed test methods, as described in [42] and [44]. The test methods were up-dated and included in the Annex "Frontal surfaces in the event of impact with a vulnerable road user proposal for test methods". Also general background information was given and choices explained. Working Group 10 has been dissolved in November 1994. A summary of the 1994 final report and an overview of the activities performed by the former members of WG10 since the end of 1994, has been presented in 1996 to the 15th ESV Conference [45]. Figure 1.11 summarises the EEVC WG10 pedestrian protection test methods.

In May 1997 the former members of EEVC WG10, on request of the EEVC Steering Committee, met again to discuss technical progress and new developments with respect to the EEVC pedestrian protection test methods. Based on these discussions the Steering Committee decided in June 1997 to set-up a new EEVC working group -WG 17 Pedestrian Safety- with two main tasks: 1. Review of the EEVC WG10 test methods (final report 1994) and propose possible adjustments taking into account new and existing data in the field of accident statistics, biomechanics and test results (to be completed within one year). Prepare the EEVC contribution to the IHRA working group on pedestrian safety.

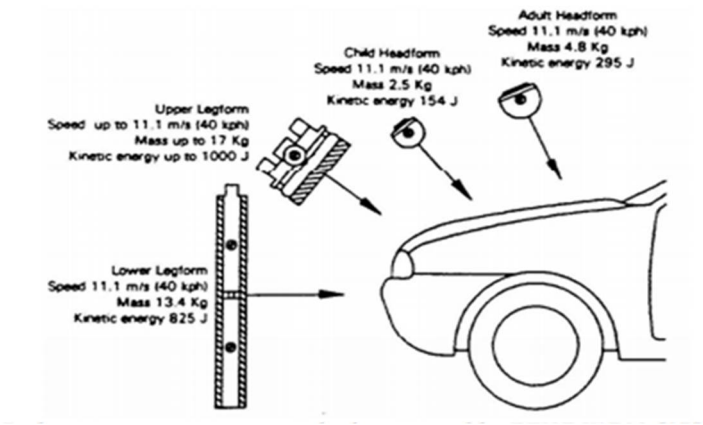

Figure 1.11 Pedestrian protection test methods proposed by EEVC WG10 [46].

The activities of WG17 with respect to the first task only are summarized in this report. New data in the field of accident statistics, biomechanics and test results are described respectively. Further improvements to the sub-system impactors are investigated.

1.6.1 Lower leg and knee

A recent study concerning the shearing and bending effects in the knee joint at high speed (i.e. 40 km/h) lateral loading was studied by WG17. When the preloaded knee joint of cadavers was exposed to a bending deformation the two most common initial damage mechanisms occurred when the knee was bent laterally at an average angle of 15° for ligament avulsion failure or at an average angle of 16° for diaphysis/metaphysis failure. When the preloaded knee joint of the cadavers was exposed to a shearing deformation the two most common initial damage mechanisms occurred at an average lateral shearing displacement of 16 mm for epiphysis failure or an average 28 mm for diaphysis/metaphysis failure. The average peak shearing force acting at the knee joint level in these latter cases was 2.4 kN and 2.9 kN respectively, while the peak bending moment in these shearing tests was 400-500 Nm [47].

The fixation method of the cadaver's femur in combination with the severity of the impacts caused extreme damage to the bones and ligaments in several cases. The most common injury

mechanisms in both the bending and the shearing test were all related to bone fractures, indicating the severity of these tests [48].

Based on the same cadaver tests an acceptance level has been proposed by JARI/JAMA, consisting of a combination of a maximum bending angle and a maximum shear displacement [49]. WG17 is not in favor of this approach since these phenomena occur at a different point in time and therefore should not be combined.

The cadaver tests discussed above confirm the lateral bending stiffness of the legform knee ligaments of 300-330 Nm, as chosen by WG10. It was already mentioned in the final WG10 report that the 100-150 Nm knee bending moments obtained from low speed cadaver tests seemed to be unrealistic [43]. This statement is confirmed by WG17.

1.6.2 Upper leg and pelvis

WG17 considered new accident reconstructions using the upper legform impactor necessary for three reasons:

- The proposed WG10 acceptance levels still had to be confirmed;
- The impactor was modified after a hidden load path was found
- There seems to be an imbalance between the current test requirements on one hand and the injury risk in real accidents with modern cars on the other hand, since modern cars do not pass the current bonnet leading edge test requirements, while few femur injuries occur in reality

The results in a dynamic test are to be static coefficient of 1.69 for the tibia bending moment to failure [50]. If this coefficient is applied to the static femur bending moment to failure of 310 Nm for male subjects (source: Messerer), this would result in a dynamic bending moment to failure of 524 Nm. The average length of male femurs is 455 mm [51]. While the µ working length of the EEVC upper legform impactor is only 310 mm. The corrected bending moment measured by the impactor

would then be 357 Nm. The French representative in WG17 proposed an acceptance level of 360 Nm for the lateral upper legform bending moment.

The JARI performed a series of 12 accident reconstructions using the upper legform impactor. Based on these tests injury risk functions for femur and pelvis AIS 2+ injuries based on lateral femur forces6 and bending moments have been developed [52]. The results seem to be influenced considerably by the age of the pedestrians. WG17 believes that the approach used results more in a fracture distribution curve rather than in an injury risk curve. Moreover, the zero risk values were chosen at a quite high level, i.e. at the WG10 acceptance levels.

WG17 recommended an injury risk level of 20%, resulting in 4.23 kN and 226 Nm for the logistic (dose-response) risk and 5.58 kN and 362 Nm for the cumulative normal risk. WG17 decided to increase the WG10 acceptance levels to the mean value of both methods. This increase in acceptance levels will contribute to a better balance between test and real accident injuries. The mean values from both methods at a 20% injury risk level are 4.9 kN and 294 Nm, which are rounded to 5.0 kN and 300 Nm respectively

1.6.3 Head

In the final report of EEVC WG10 [44]. The following sentence is included Confirmation is still necessary for the child acceptance level of 1000, although it is mentioned in literature that a HIC value of 1000, when used with the NHTSA head impact system, was verified as an accurate indicator of the threshold of serious head injury through experimental reconstruction of real pedestrian cases involving adults and children. Recently NHTSA has evaluated different techniques for developing child dummy protection values [14]. Several techniques, including scaling of adult data and accident reconstructions, have been evaluated and it was concluded that no single method or set of data stands out clearly as the best choice, because actual biomechanical data are insufficient and of limited applicability. Therefore it is recommended by NHTSA to use HIC 1000 for a 6-yr

child, since this value has been an established limit for both adult and child dummies for many years, and is proven to be effective in limiting serious injury. WG17 accepted this NHTSA recommendation. ISO/TC22/SC12/WG6 is currently discussing the HIC protection value for children and this may lead to new considerations.

1.6.4 EEVC dynamic testing criteria

The performance of real vehicles with respect to the EEVC test methods has been evaluated by WG17 in several programmes. Computer simulations are used more and more in the development process of new vehicles or components. Computer simulations were also used by WG17, beside dummy and cadaver tests, to define the input conditions for the sub-system impactor tests. Recently streamlined cars seem to indicate that the impact energy of the currently described upper legform to bonnet leading edge test is too high for these vehicle shapes. A proposed requirements made by EEVC for dynamic testing is shown in Table 1.4.

Table 1.4 EEVC dynamic testing criteria [45].

Value	Lower Limit	Upper Limit
Tibia Acceleration [g]	120	250
Bending Angle [degree]	6.2	8.2
Shearing Displacement [mm]	3.5	6.0

1.6.5 Structure of the legform impactor and its modeling

Considering previous studies and other legform impactors that have been used for pedestrian safety analyses, there are some points that should be considered e.g. similar legform impactor models are often commercial and no precise relevant engineering data are available for use by other researchers the geometrical and mechanical properties of different parts and the method for modeling a legform impactor are described in detail for the first time in the literature.

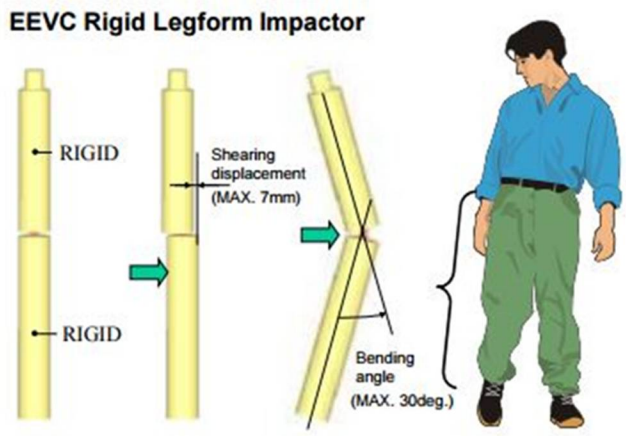

Figure 1.12 EEVC pedestrian subsystem impact test features (EEVC/WG17) [45].

The main idea in our proposed legform impactor model is to introduce a simple model using a few components to achieve acceptable results in a relatively short time. In some legform impactor models, the results achieved in the required standard static and dynamic tests are not applicable to the whole range of applications.

Pedestrian protection is a worldwide concern, especially in European countries. The European Enhanced Vehicle Safety Committee (EEVC/WG10 and WG17) proposed a component subsystem test for cars to assess pedestrian protection [19].

To determine the aggressiveness of a bumper using a legform impactor, impact is imposed at 40 km/h horizontally in line with the automobile. The lower leg acceleration, knee shearing displacement and knee bending angle are measured. A pedestrian subsystem impact representation shown in Figure 1.10. The femur and tibia are represented by two cylinders, each of 70 mm outer diameter. The geometrical properties of the femur and tibia, such as mass, moments of inertia and center of gravity, are specified in the EEVC/WG17 report [19]. The femur and tibia are covered by artificial flesh and skin. *MAT_FU_CHANG_FOAM are used for modeling the flesh and skin, respectively.

1.7 Summary

The threshold and injury criteria used in research on pedestrian safety are summarized in Table 1.5, based on the results from extensive studies in the past three decades. All these tolerance levels are the acceptance levels of EEVC proposal and from the European Passive Safety Network [23].The injury related parameters can be used for evaluation the safety performance of the vehicle front structures. The HIC value is the most commonly used criterion for head injury in crash safety research and used also for assessment of risk of pedestrian head/brain injuries for many years. Further, Institutes like EEVC are studying the material properties of human tissues in dynamic conditions [23].

Table 1.5 The threshold and injury criteria for pedestrian body segments [2].

Parameter	Body Segments	Tolerance levels
Force	Tibia	4 kN
	Knee	2.5 kN
	Femur	kN
	Pelvis	4 kN
HIC	Adult	<1000
	Child	<1000
Linear Acceleration	Head	80g
	Thorax	60g
	Tibia	150 g
Angular Acceleration	Head	3000 rad/s2
Rotation Angle	Knee	15 deg
	Neck	60 deg
Bending Moment	Knee	350 Nm
	Tibia	200 Nm
	Femur	220 Nm
Shear Dislocation	Knee	6 mm

CHAPTER 2

OBJECTIVE AND METHODOLGY

2.1 Objective

A pedestrian injury risk in a collision with car model is related to several parameters, such as vehicle design and its structure, vehicle high speed and the direction of the car movement. To improve pedestrian protection in various circumstances, finite element modeling and simulation can represent to evaluate the vehicle and pedestrian collision.

The objective of this research is to carry out an analysis of legform impactor collision with a finite element car model and compare with multibody models. The injuries sustained by knee and interms of its displacement, bending angle and acceleration are obtained using different workbenches. The explicit LS-DYNA code is used to verify the vehicle performance against the biomechanical limits. The MADYMO biodynamic simulation software, which is widely used in the automobile industry, is used to develop the models and perform the crash simulations.

The research concentrates on following specific aims:

1. To evaluate a legform impactor model impacted on the frontal side of the car at a velocity of 40 km/h in a direction parallel to the longitudinal axis of the vehicle.
2. To evaluate the values of the injury parameters and determine the same using EEVC/EG17 criteria in MADYMO simulation code.
3. To investigate an ellipsoidal, 50th pedestrian dummy model under same impacted conditions.
4. To evaluate the values of injury parameters at two different impact speeds of 40 kmh, 27 kmh.
5. To evaluate and compare the most crucial factors affecting lower leg injuries such as

lower leg acceleration, knee shearing displacement, and knee bending angle by using the mathematical models developed in Ls-Dyna and Madymo (EEVC/WG17).

2.2 Methodology

To determine the stability of a car model using a legform impactor, impact is imposed at 40 km/h horizontally in line with the stationary vehicle model. The lower leg acceleration, knee shearing displacement and knee bending angle are measured

Lower leg impact models are impacted laterally at the front of the vehicle. Evaluation of the proposed pedestrian legform model was done by comparing the results obtained from the LS-Dyna and MADYMO analysis for a pedestrian-car impact with those obtained from the experiments with test performed. A schematic representation of method used in this study shown in Figure 2.1, where injuries made by lower extremist are compared on different workbenches.

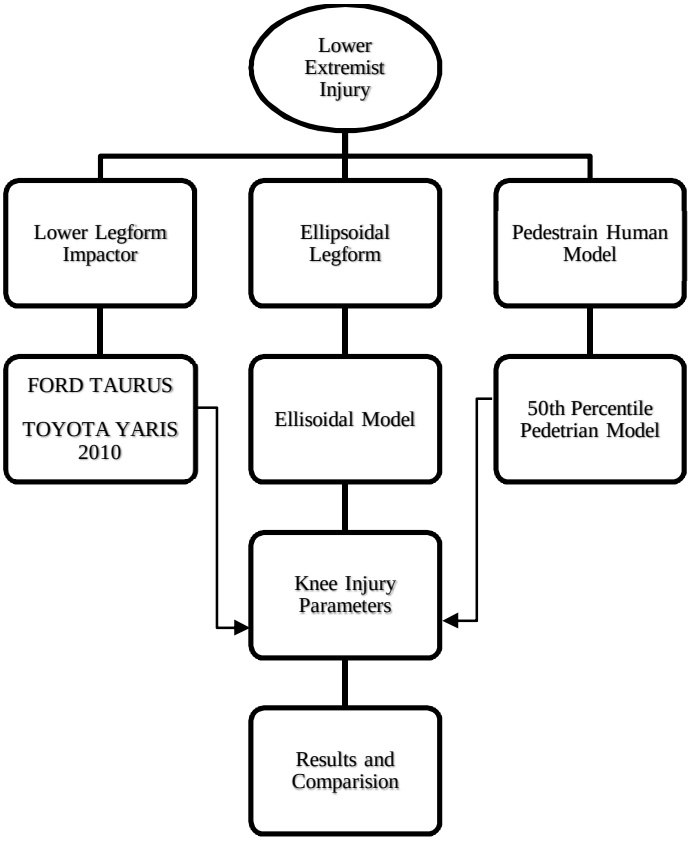

Figure 2.1 Methodology flow chart for this research.

2.2.1 Finite element method

To begin an impactor-vehicle collision, such as the CAD design and model representation are needed to be developed. The legform impactor model is obtained from the Livermore Software Technology Corporation (LSTC) and the vehicle model taken from National Crash Analysis Center (NCAC) [53]. Making the FE discrete models organized, the respective models need to be verified the parameters that encompasses the regulation criteria EEVC EG17. The explicit code are run to verify the vehicle performance against the criteria and simulation of the collision between the car and impactor .The impactor responses which represents the lower extremity can that be determined. The simulations depict crucial results related to the lower extremity injuries, which is especially important in the evaluation of legform model. As the impactor model striking the car model lead to ligament injuries, the friction forces may cause the pedestrian to be moved aside in front of the car model. Although kinematics of the legform is slightly different, the results from the full size pedestrian model is used for further evaluated and compared.

2.2.2 Multibody method

Although the current criteria of the legform impactor is used for vehicle manufactures to determine the grades and ratings of the car model the results might be slightly different from actual the kinematics of an impacted pedestrian. This study makes multi-body models and simulations by means of MADYMO (Mathematical Dynamic Modelling) for the vehicles with high bumpers and high front end to match the same geometry as of FE models. Same parameters like speed, position are implemented in multi body approach to verify with Finite element analyses

The assumptions of the multibody models is that their system points may be represented as rigid. The kinematics joints between the segments are often specified with functions such as friction and damping. The main frontal side of the vehicle parts are crucial to verify the motion and response

of the pedestrian therefore the multi body model does not require large parameters strain curves, contact cards as of FE approaches.

2.3 Computational Test Matrix

To investigate the pedestrian-vehicle collision, the legform sub-system or the full-sized pedestrian is impacted at 27 km/h and 40 km/h horizontally in line with the stationary vehicle model. The lower leg acceleration, knee shearing displacement and knee bending angle are measured shown in table 2.1

Table 2.1 Computational test matrix

Legform/Pedestrian Models	Vehicle -Model	Impact Velocity (km/h)
FE Impactor	Ford Taurus	27 km/h
FE Impactor	Toyota Yaris	27 km/h
FE Impactor	Ford Taurus	40 km/h
FE Impactor	Toyota Yaris	40 km/h
Ellipsoidal Impactor	Ellipsoidal Car	27 km/h
Full-size Pedestrian	Ellipsoidal Car	27 km/h
Ellipsoidal Impactor	Ellipsoidal Car	40 km/h
Full-size Pedestrian	Ellipsoidal Car	40 km/h

2.4 MADYMO Crash Simulation

2.4.1 Introduction to MADYMO

MADYMO (Mathematical Dynamic Models) is a software package that allows users to design and optimize the crash safety performance of vehicles efficiently, quickly, and cost- effectively [29]. It is generic multibody and finite element software with a range of specific features for impact simulation. MADYMO provides analysis in the time domain based on explicit integration techniques. It is used extensively in design and engineering companies and departments, as well

as research laboratories and universities. MADYMO has proven its value in numerous fields of application, often supported by verification studies using experimental test data. While automotive safety is MADYMO's main field of application, other markets include biomechanical research; comfort analysis; bus, truck and train safety; vehicle dynamics; sports.

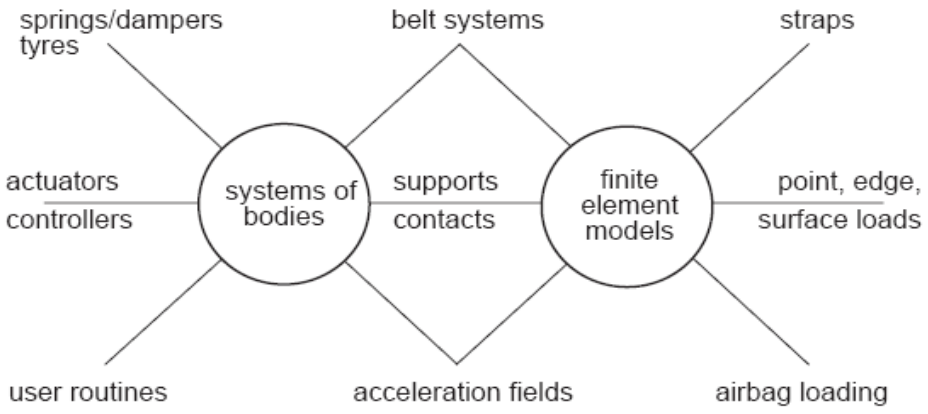

Figure 2.2 MADYMO 3D structure [29].

MADYMO combines in one simulation program the capabilities offered by multi-body (for the simulation of the gross motion of systems of bodies connected by kinematical joints) and finite element techniques (for the simulation of structural behavior) Figure 2.2 shows the structure of MADYMO Software code. A model can be created with only finite element models, or only multi-bodies, or both**.**

The multi-body algorithm in MADYMO yields the second time derivatives of the degrees of freedom in an explicit form. The number of computer operations is linear in the number of bodies if all joints have the same number of degrees of freedom. This leads to an efficient algorithm for large systems of bodies. At the beginning of the integration, the initial state of the systems of bodies has to be specified in terms of joint positions and velocities. Several kinematic joint types are available with dynamic restraints to account for joint stiffness, damping and

friction. Joints can be locked, unlocked or removed based on user-defined circumstances.

The approach that the interaction between bodies and finite elements is modeled allows the use of different time integration methods for the equations of motion of the finite element part and the multi-body part. The integration methods used are conditionally stable and therefore put limitations on the maximum time step that can be used. To increase the efficiency of the entire analysis, the finite element module can be sub-cycled with respect to the multi-body module using different time steps for each module.

Multibody elements in MADYMO can be separated into three groups, viz; the inertial system, multibody system and the null system. The elements used to model the seat, floor and other immovable objects belong to the inertial system. The elements that are affected by acceleration fields and contact forces are included in the multibody system. The Anthropomorphic Testing Device (ATD) is an example of this type of system.

A typical crash model consists of an ATD as a multibody system placed in a seat that forms a part of the inertial space. Multibody systems are usually connected by joints.

2.4.2 Multibody systems

A multi-body system is a system of bodies. Any pair of bodies in the same system can be interconnected by one kinematic joint. The MADYMO multi-body formalism for generating the equations of motion is suitable for systems of bodies with a tree structure and systems with closed chains. Systems with closed chains are reduced to systems with a tree structure by removing a kinematic joint in every chain. Removed joints are subsequently considered as "closing" joints. For each (reduced) system with a tree structure, one body can be connected to the reference space by a kinematic joint, or the motion relative to the reference space of one body can be prescribed as a function of time.

Several multi-body systems can be defined in MADYMO. A multibody system is a set of

bodies interconnected by kinematic joints. Two sets of bodies are separate multi-body systems when there are no kinematic joints between the two sets. The interconnection structure of a multi-body system is implicitly defined in the input file. Kinematic joints connect the bodies and define the structure of the multi-body system.

2.4.3 Kinematic joints

A kinematic joint restricts the relative motion of the two bodies it connects. A specific type of kinematic joint is characterized by the way the relative motion of two bodies is constrained. The relative motion allowed by a joint is described by quantities called joint degrees of freedom. The number depends on the type of joint. In MADYMO, the most common joint types are available such as spherical joints, translational joints, revolute joints, cylindrical joints, planar joints and universal joint.

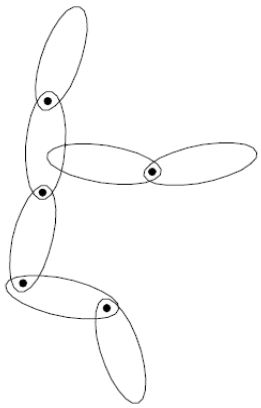

Figure 2.3 Examples of single and multibody systems with tree structure [29].

A system of bodies is defined by: -1) the bodies: the mass, the inertia matrix and the location of the centre of gravity, 2) the kinematic joints: the bodies they connect, the type, and 3) the location and the orientation, and 4) the initial conditions. Figure 2.3 shows the tree structure of multibody system. In addition, the shape of bodies may be needed for contact calculations or post processing (graphics) purposes. Applied loads on bodies can be modeled with the force models described in the following chapters.

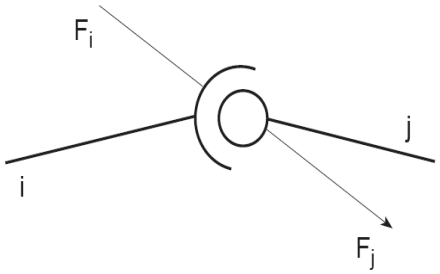

Figure 2.4 Constraint load in a spherical joint [29].

A kinematic joint shown in Figure 2.4 is referred to by the number of the child body of the two bodies connected by the joint. The constraints imposed by a kinematic joint cause a load on the pair of interconnected bodies, the constraint load.

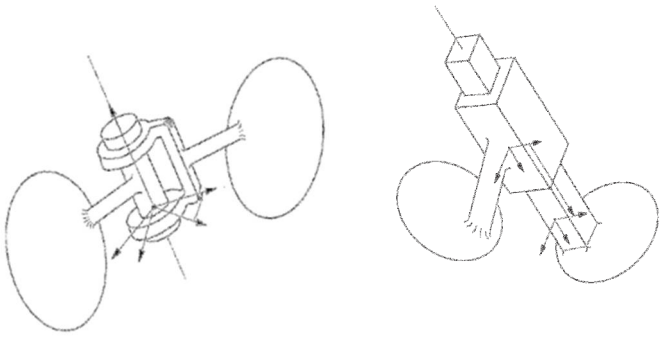

Revolute Joint Translational Joint

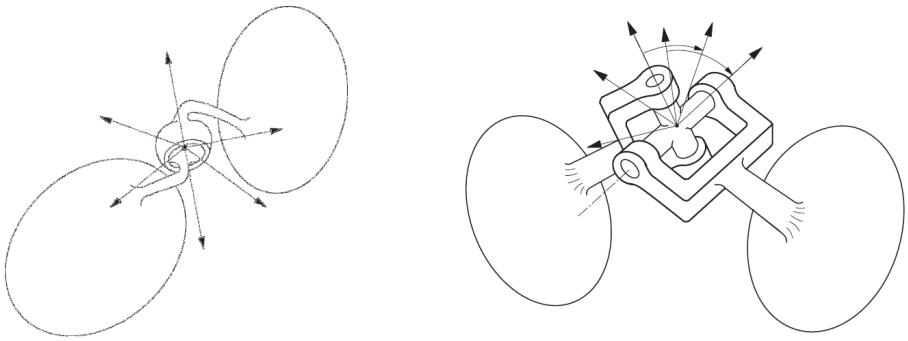

Spherical Joint Universal Joint

Figure 2.5 Different types of joints [29].

This load is such that the relative motion of the pair of bodies is restricted to a motion that does not violate the constraints imposed by the kinematic joint. The constraint loads on the separate bodies are equal but opposite loads. Constraint loads can be used to assess the strength of the joint.For every type of kinematic joint there corresponds a dynamic joint model. Different types of joints shown in Figure 2.5. It is a force model that defines the elastic, damping and friction loads that depend on the relative motion in the kinematic joint. For most types of joints, an elastic, damping and friction load can be specified for every joint degree of freedom. The load is either a force or a torque depending on whether the joint degree of freedom is a translation or a rotation, respectively.

2.4.4 Force interactions

MADYMO offers a set of standard force accelerations and contacts of bodies with each other or their surroundings. These are discussed in the following subsections. Figure 2.6 gives a clear and concise idea of this concept. Finite element structures can be used for the driver, passenger side airbag and the knee bolster. An input data file is then set up which specifies the mass distribution of the bodies, the connections between the bodies and the joint properties, and for finite element structures.

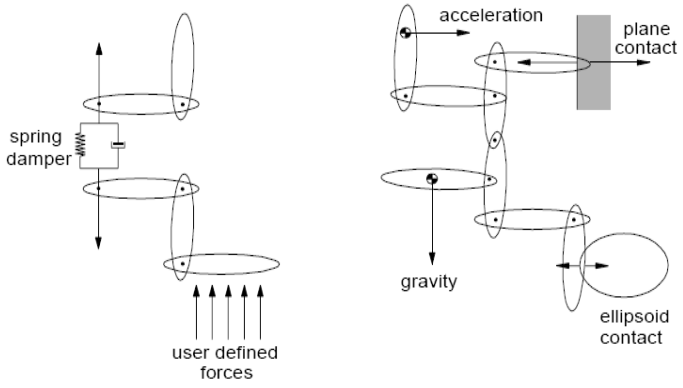

Figure 2.6 Examples of systems of bodies with force interactions [29].

2.4.5 MADYMO ATD databases

Simulations are done using well validated ATD databases. Two dimensional and three dimensional databases of ATD models are available in MADYMO. A broad range of MADYMO ATD models are available. The standard models of the child and adult hybrid III dummies are 3-year-old child, 6-year-old child, 5th percentile female, 50th percentile male and 95th percentile male hybrid III dummy models. The 50th percentile male ATD hybrid dummy represents an "Average" of the USA adult male population. Different dummy model and its size available in MADYMO database shown in Figure 2.7.

Two other versions of the Hybrid III have been developed, the 5th percentile small female and the 95th percentile large male. In this research, the 6-year-old child dummy, 5th percentile female hybrid III dummy, the 50th percentile male Hybrid III dummy, and 95th percentile male Hybrid dummy is used.

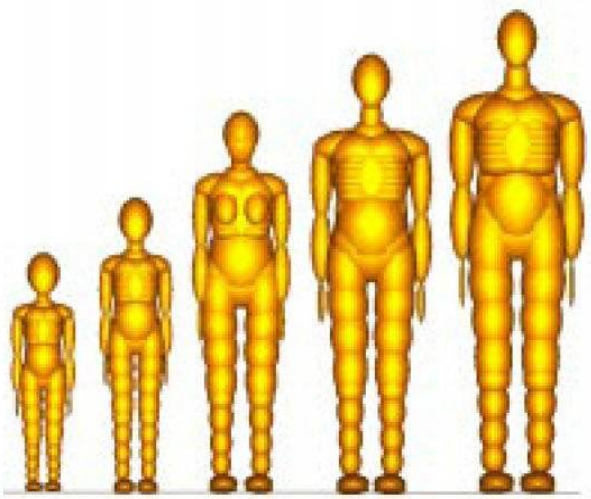

Figure 2.7 MADYMO pedestrian models [29].

Pedestrian models each consists of 52 rigid bodies, in 7 configuration branches. The outer surface is described by 64 ellipsoids and 2 planes. Comparison of weight and geometry for the

HYBRID III family dummies shown in Table 2.1.The data for the dimensions of the ellipsoids are determined from technical drawings at TNO. It is possible to adjust the dimensions if necessary for a more adequate description of the contacts. The child Hybrid III dummy models have same characteristics which were derived by scaling those of the 50th percentile male Hybrid III model.

Table 2.2 Weight and geometry information for Hybrid III family ATD's [29].

Comparison of Weight, Sitting Height, and Structure for HYBRID III Family					
	12 mo CRABI	**3 YO Child**	**6 YO Child**	**5% Female**	**50% Male**
Weight (lb)	22.0	34.1	51.6	108.0	172.3.0
Stature (in)	29.4	37.2	45.0	59.1	69.0
Sitting Height (in)	18.9	21.5	25.0	31.0	34.8

2.5 LS DYNA

LS-DYNA is a highly advanced general purpose nonlinear finite element program that is capable of simulating complex real world problems. The distributed and shared memory solver provides very short turnaround times on desktop computers and clusters operated using Linux, Windows, and UNIX. With LS-DYNA, Livermore Software Technology Corporation (LSTC) aims to provide methods to seamlessly solve problems requiring [54]. LS-DYNA is a general-purpose finite element program capable of simulating complex real world problems. It is used by the automobile, aerospace, construction, military, manufacturing, and bioengineering industries. LS-DYNA is optimized for shared and distributed memory Unix, Linux, and Windows based, platforms, and it is fully QA'd by LSTC. The code's origins lie in highly nonlinear, transient dynamic finite element analysis using explicit time integration. "Nonlinear" means at least one (and sometimes all)

of the following complications: Changing boundary conditions (such as contact between parts that changes over time) Large deformations (for example the crumpling of sheet metal parts).

Nonlinear materials that do not exhibit ideally elastic behavior (for example thermoplastic polymers) "Transient dynamic" means analyzing high speed, short duration events where inertial forces are important. Typical uses include: Automotive crash (deformation of chassis, airbag inflation, seatbelt tensioning), Explosions (underwater Naval mine, shaped charges), Manufacturing (sheet metal stamping), LS-DYNA's potential applications are numerous and can be tailored to many fields. In a given simulation, any of LS-DYNA's many features can be combined to model a wide range of physical events. An example of a simulation, which involves a unique combination of features, is the NASA JPL Mars Pathfinder landing simulation which simulated the space probe's use of airbags to aid in its landing. LS-DYNA is one of the most flexible finite element analysis software packages available [55].

LS-DYNA consists of a single executable file and is entirely command line driven. Therefore, all that is required to run LS-DYNA is a command shell, the executable, an input file, and enough free disk space to run the calculation. All input files are in simple ASCII format and thus can be prepared using any text editor. Input files can also be prepared with the aid of a graphical preprocessor.

There are many third party software products available for preprocessing LS-DYNA input files. LSTC also develops its own preprocessor, LS-Pre Post, which is freely distributed and runs without a license. Licensees of LS-DYNA automatically have access to all of the program's capabilities, from simple linear static mechanical analysis up to advanced thermal and flow solving methods. Furthermore, they have full use of LS-OPT, a standalone design optimization and probabilistic analysis package with an interface to LS-DYNA.

CHAPTER 3

FE LEGFORM AND VEHICLE FE MODELING AND IMPACT ANALYSIS

3.1 FE Legform Model

The multi-body chain (bodies, joint and joint restraints) forming the core of the FE model is identical to that of the ellipsoid model. However, in the FE model the foam and skin that cover the steel tubes are modelled explicitly, with SOLID8 finite element meshes. MATERIAL.FOAM is used to model the foam and skin material properties. A typical FE Legform model shown in Figure 3.1 [55].

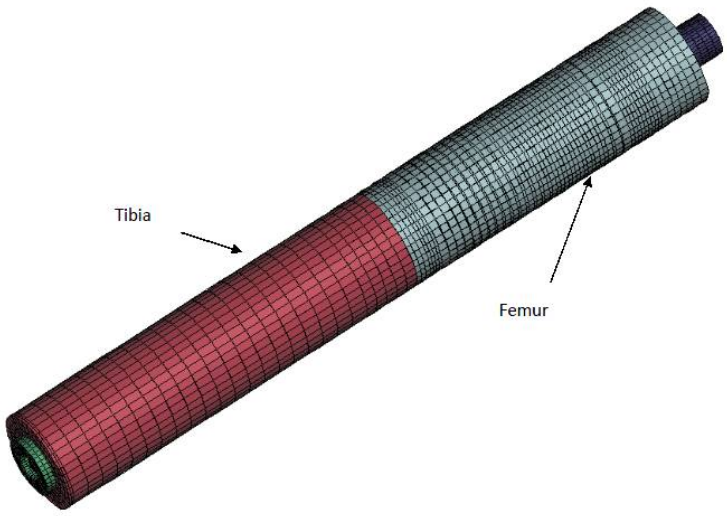

Figure 3.1 The FE legform model [55].

The FE legform model geometry as well as the combined rigid body and finite element inertia properties, are defined such that all the EEVC-WG17 design specifications are met. The outer surfaces of the steel femur and tibia tubes are modelled with fully supported MEM4 meshes with MATERIAL.NULL (facet surfaces). The foam to steel load transfer is modelled with a

contact definition using CONTACT.FE_FE. The legform impactor output definitions are included in the same way as in the ellipsoid model.

To evaluate the legform impactor, the EEVC/ WG17 dynamic test guidelines were used. The bones of the femur and tibia of the legform impactor were modeled using shell elements. After modeling the geometry of the legform impactor for achieving the required mass, two lump masses in special locations were used to tune the masses in the center of gravity of the femur and tibia. As specified in EEVC/WG17, the total masses of the femur and tibia shall be (8.6±0.1) kg and (4.8±0.1) kg, respectively.

The particular problem here is the characteristics of the knee joint between the femur and tibia and those of the foam and skin. The knee joint was modeled using a 6-DOF discrete beam. The shearing of the knee was represented by a linear force-versus displacement curve and the bending response of the Upper legform impactor Headform impactor (Child) (Adult) Lower legform impactor Fig. 1 EEVC pedestrian subsystem impact test features (EEVC/WG17) Standard measurement parameters (EEVC/WG17) knee was represented by a nonlinear moment-versus rotational-displacement curve. Different degrees of freedom of the knee joint were tuned so that the static and dynamic characteristics were achieved.

3.2 Vehicle FE Models

In this thesis study, the pedestrian impact responses against typical passenger cars are examined. In the process, two vehicle models one a midsize sedan (Ford Taurus), and another a small side (Toyota Yaris), are considered and potential pedestrian injuries are investigated.

3.2.1 Ford Taurus model

A finite element (FE) model of a 2001 Ford Taurus was developed at the National Crash Analysis Center (NCAC) of The George Washington University (GWU) under contract with the

Federal Highway Administration (FHWA) for studying and advancing vehicle and highway safety research [53]. Reverse engineering methods were employed to build a detailed FE model suitable for different crash conditions. This model has been periodically updated and enhanced to include more detail and improve robustness. Details and description of model is shown in Figure 3.2.

Year	2001
Model	Ford Taurus
Class	Midsize
Weight (Kg)	1578.5
Wheel Base (mm)	2760.4
Total No of Elements	981,092

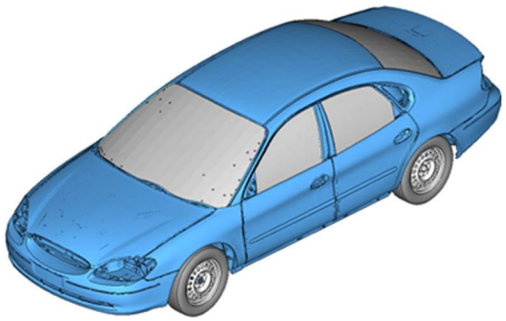

Figure 3.2 Ford Taurus model [53].

3.2.2 Toyota Yaris model

A finite element (FE) model based on a 2010 Toyota Yaris passenger sedan was developed through the process of reverse engineering at the National Crash Analysis Center (NCAC) of The George Washington University (GWU) [53]. These efforts were conducted under a contract with the Federal Highway Administration (FHWA). This model will become part of the array of FE

models developed to support crash simulation. The model was validated against the National Highway Traffic Safety [53].

Administration (NHTSA) frontal New Car Assessment Program (NCAP) test for the corresponding vehicle. This vehicle was selected for modeling to reflect current automotive designs and technology advancements for an important segment of the vehicle fleet. This model is expected to support current and future NHTSA research related to occupant risk and vehicle compatibility as well as FHWA barrier crash evaluation, research, and development efforts. Details and description of model is shown in Figure 3.3.

Year	2010
Model	Toyota Yaris
Class	Compact
Weight (Kg)	1137.6
Wheel Base (mm)	2538
Total No of Elements	1,519,181

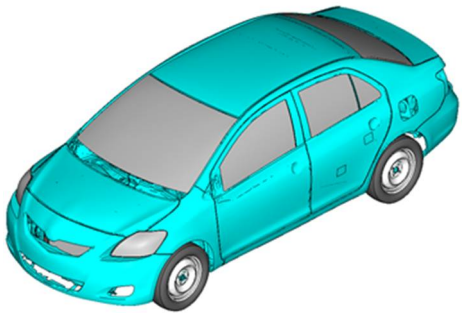

Figure 3.3 Toyota Yaris model [53].

3.3 Fe Legform and Vehcile Model Simulations Results

Results are presented separately for each vehicle, followed by a comparison of injury parameters. Peak Injury measurements are compared to EEVC requirements. Time histories for all test are kept constant in order to verify the responses on different models. The FE model cars are verified with EEVC limits for the impact to the center bumper only.

3.3.1 Kinematics of FE legform simulation with Ford Taurus at 27 kmh

The legform-car model impact was imposed at 27 kmh velocity parallel to the longitudinal axis of the vehicle, and initial conditions of analyses were as mentioned in EEVC working group 17. Figure 3.4 shows the legform-car model collision. In the FEM of these analyses, the frontal side of the car model is completed with all necessary joints and welding to make the bumper, hood, beam other components more stiff to correspond to the collision with impactor. An impact was imposed on the center of the bumper and three important parameters of the legform were recorded. According to the EEVC/WG17 pedestrian test, the maximum permitted knee bending angle criterion, knee shearing displacement and upper tibia acceleration are 15°, 6 mm and 150g respectively.

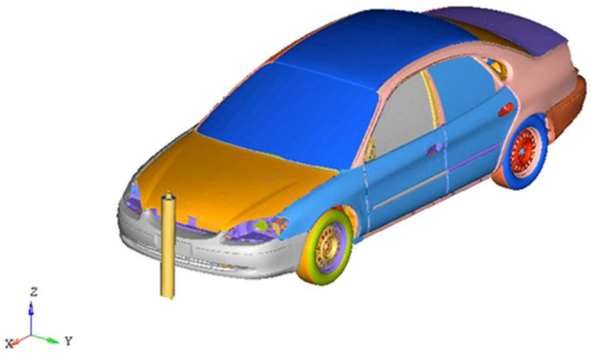

Figure 3.4 Legform impact with car model at 27 kmh

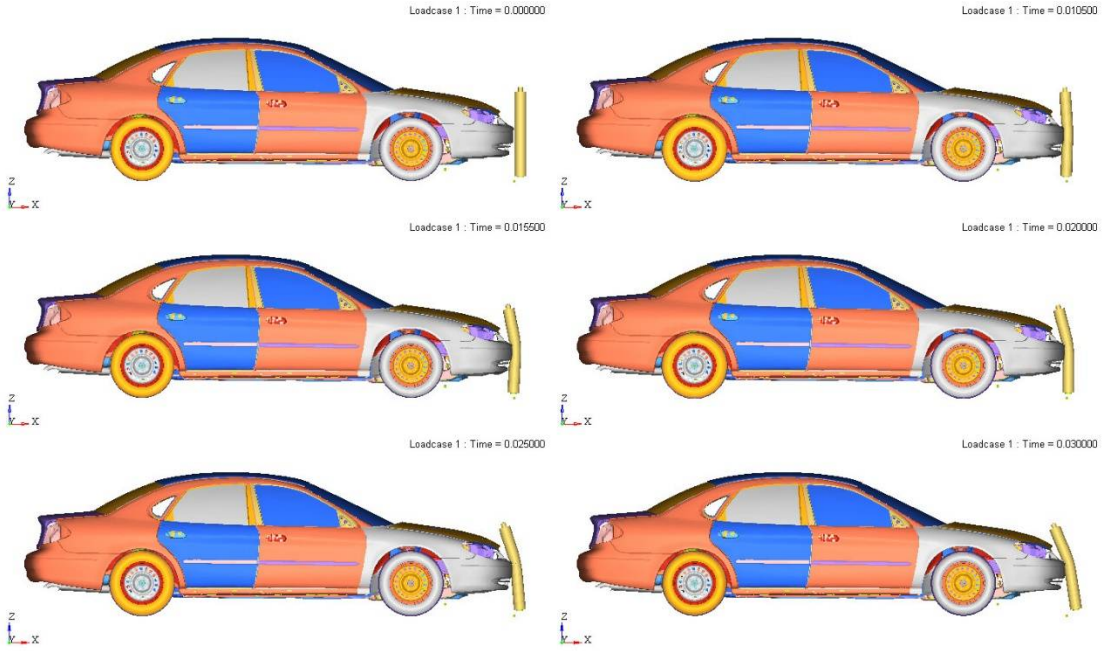

Figure 3.5 Legform collision with Ford Taurus at 27 kmh

A post and pre simulation of Ford Taurus is depicted in Figure 3.6, as it is performed on lower legform impactor to verify that its performance is within EEVC criteria limit. Since the legform model consist of rigid bodies connected by joints, and finite elements the knee joint is more effect in the whole simulation.

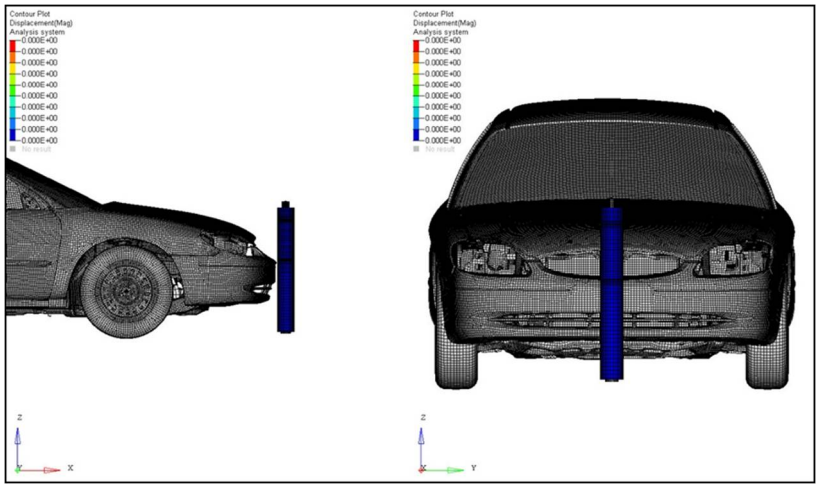

Figure 3.6 Post and pre-simulations of Ford Taurus

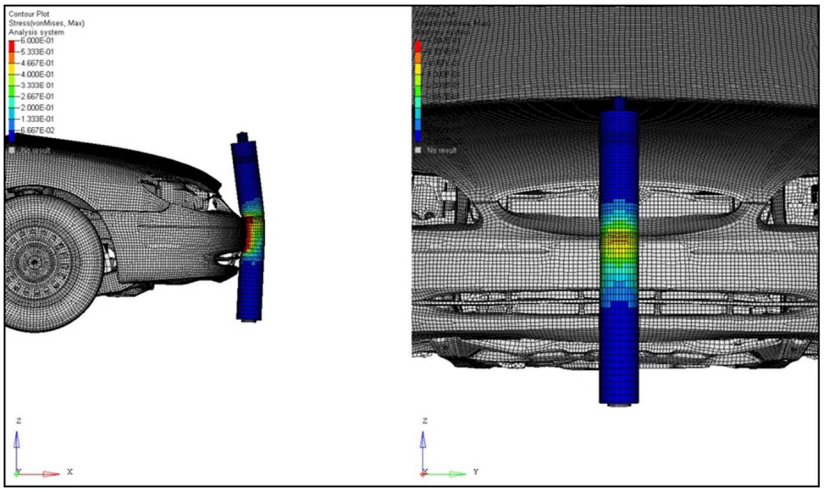

Figure 3.6 (continued)

The knee bending angle in legform impactor when strikes with Ford Taurus model at 27 kmh analyses is shown in Figure 3.5. The maximum knee bending angle in the car model was within the EEVC acceptable criteria and by changing the position, material and increasing the velocity of the impactor, the maximum knee bending angle can also be increased.

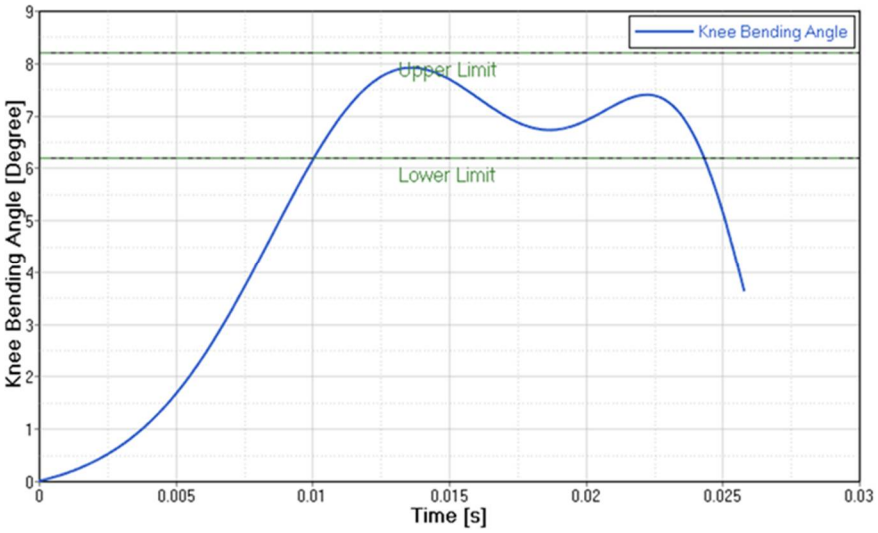

Figure 3.7 Maximum knee bending angle at initial velocity 27 kmh

The maximum bending angle obtained as 7.7 for a run of 30ms. As the strength of the bumper beam was increased, the bumper assembly resisted free movement and the bending angle

in the legform increased. In above analyses, the maximum knee bending angle occurred at 10-12 ms after its collision. The simulation result in shown in Figure 3.7

The knee shear displacement from the above analyses are shown in Figure 3.8 respectively. The knee shearing displacement was within the EEVC acceptable criteria with displacement done by potentiometer. The knee shearing displacement is corresponds to the bumper design and its stiffness of the material used. The knee shear displacement for the above analyses is obtained as 5.4mm for a run of 30ms.

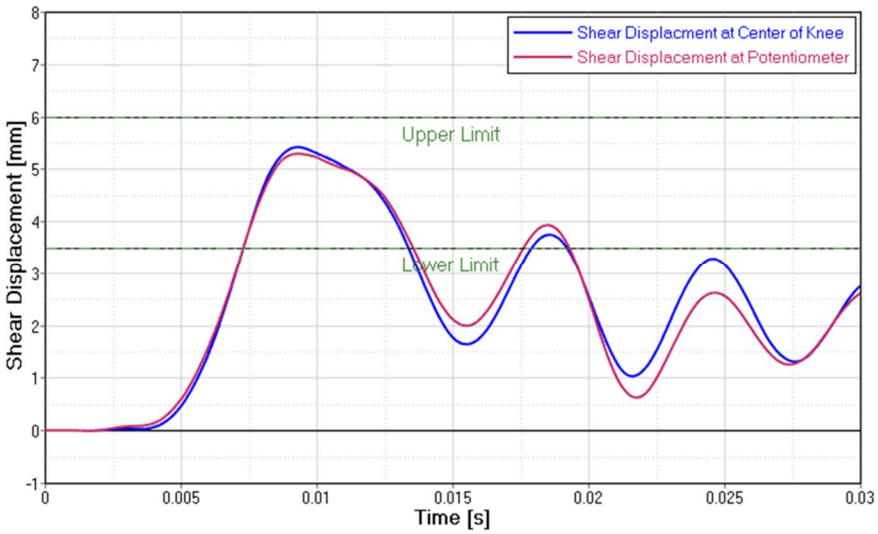

Figure 3.8 Maximum shear displacement at 27 kmh

Tibia acceleration responses is shown in Figure 3.9. Upper tibia acceleration increases if the strength of the car model is more stable to respond the collision. The tibia acceleration gives the result as soon as the collision occurs with car model. The maximum acceleration obtained for this analyses is 202g for a run of 30ms.

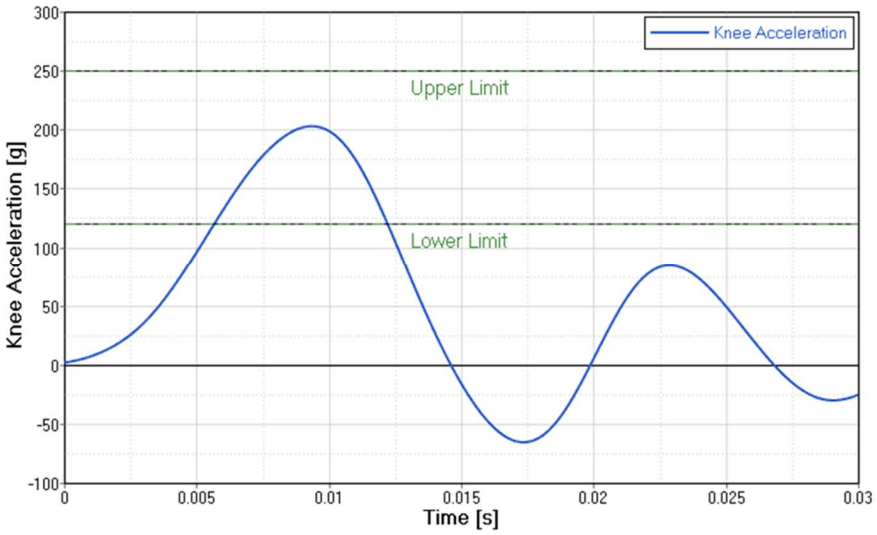

Figure 3.9 Maximum tibia acceleration at initial velocity 27 kmh

3.3.2 Kinematics of FE legform simulation with Ford Taurus at 40 kmh

The legform-car model impact was imposed at 40 km/h velocity parallel to the longitudinal axis of the vehicle, and initial conditions of analyses were as mentioned in EEVC working group 17. Figure 3.10 shows the legform-car model collision.

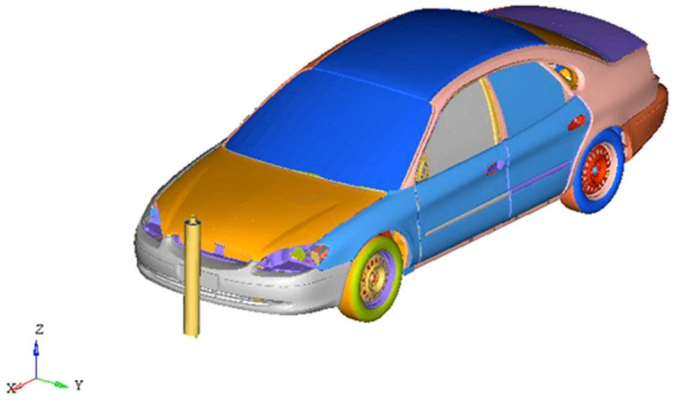

Figure 3.10 Legform impact with car model at 40 kmh

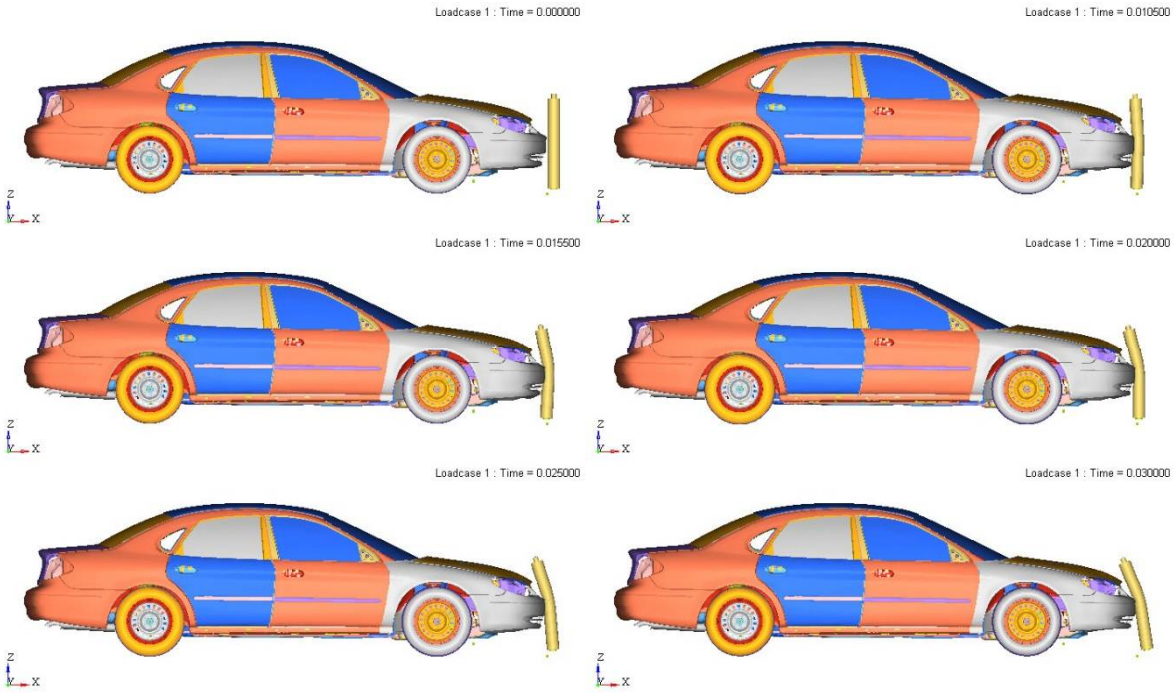

Figure 3.11 Legform collision with Ford Taurus at 40 kmh

The knee bending angle in legform impactor when strikes with ford Taurus model at 40 kmh analyses is shown in Figure 3.11.

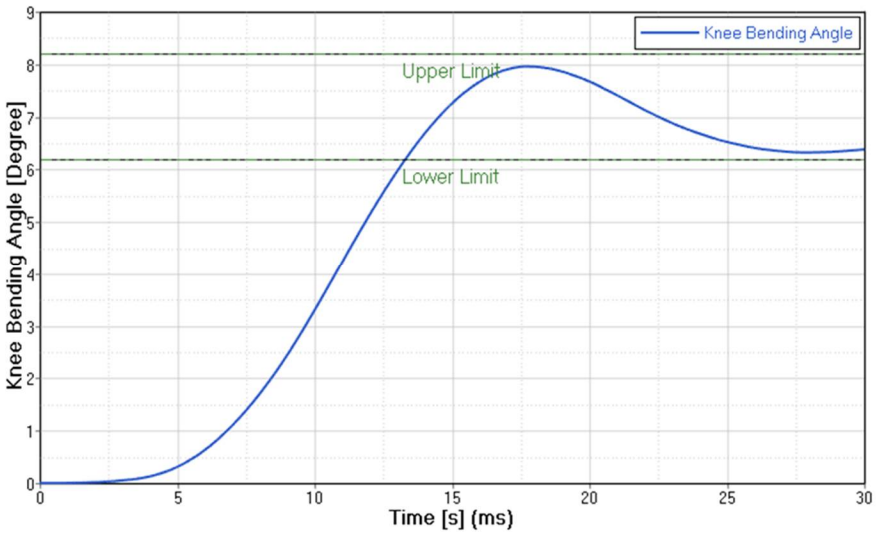

Figure 3.12 Maximum knee bending angle at initial velocity 40 kmh

The maximum knee bending angle in the car model was within the EEVC acceptable criteria and by changing the position, material and increasing the velocity of the impactor, the maximum

knee bending angle can also be increased. The maximum bending angle obtained as 7.9 for a run of 30ms. As the strength of the bumper beam was increased, the bumper assembly resisted free movement and the bending angle in the legform increased. In above analyses, the maximum knee bending angle occurred at 9-11 ms after its collision. The simulation result in shown in Figure 3.12 respectively.

The knee shearing displacement was within the EEVC acceptable criteria with displacement done by potentiometer. The knee shearing displacement is corresponds to the bumper design and its stiffness of the material used. The knee shear displacement for the above analyses is obtained as 5.2mm for a run of 30ms shown in Figure 3.13.

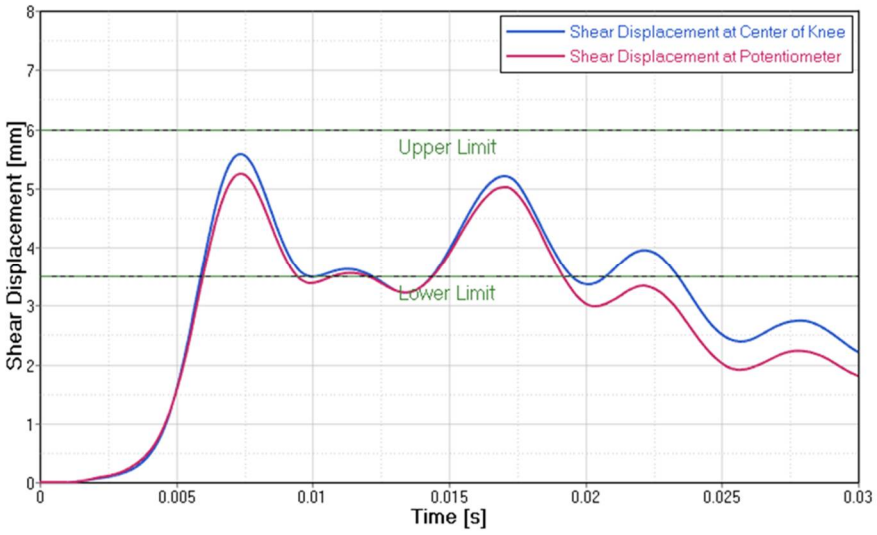

Figure 3.13 Maximum shear displacement at 40 kmh

Tibia acceleration analyses is shown in Figure 3.14. The upper tibia acceleration increases if the strength of the car model is more stable to respond the collision .the tibia acceleration gives the result as soon as the collision occurs with car model .the maximum acceleration obtained for this analyses is 201g for a run of 30ms.

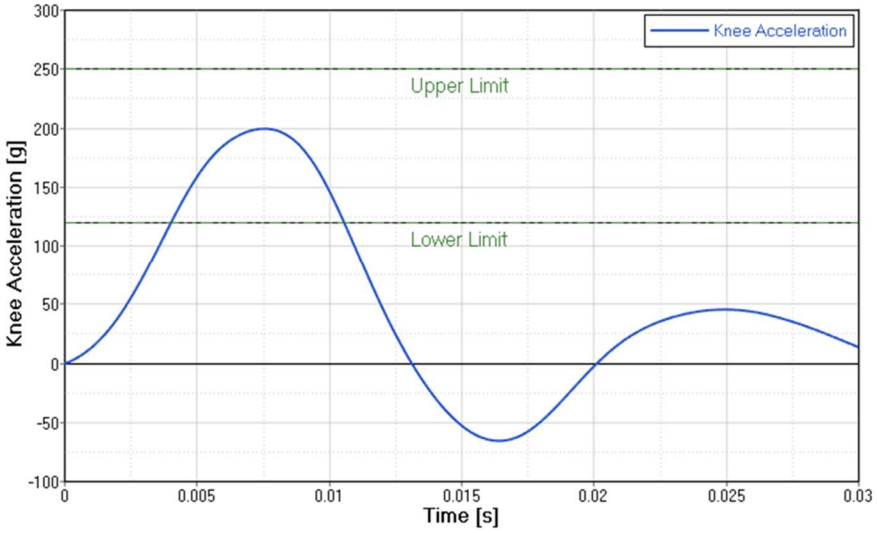

Figure 3.14 Maximum tibia acceleration at initial velocity 40 kmh

3.3.3 Kinematics of FE legform simulation with Toyota Yaris at 27 kmh

The legform-car model impact was imposed at 27 kmh velocity parallel to the longitudinal axis of the vehicle, and initial conditions of analyses were as mentioned in EEVC working group 17. Figure 3.15 shows the legform-car model collision.

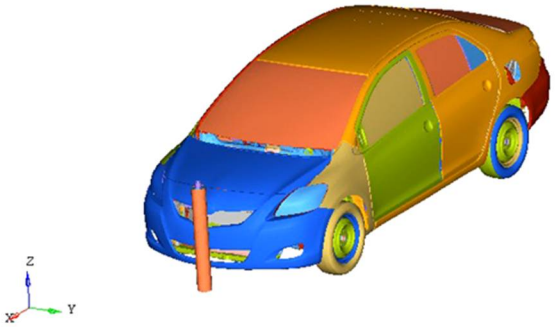

Figure 3.15 Legform impact with car model at 27 kmh

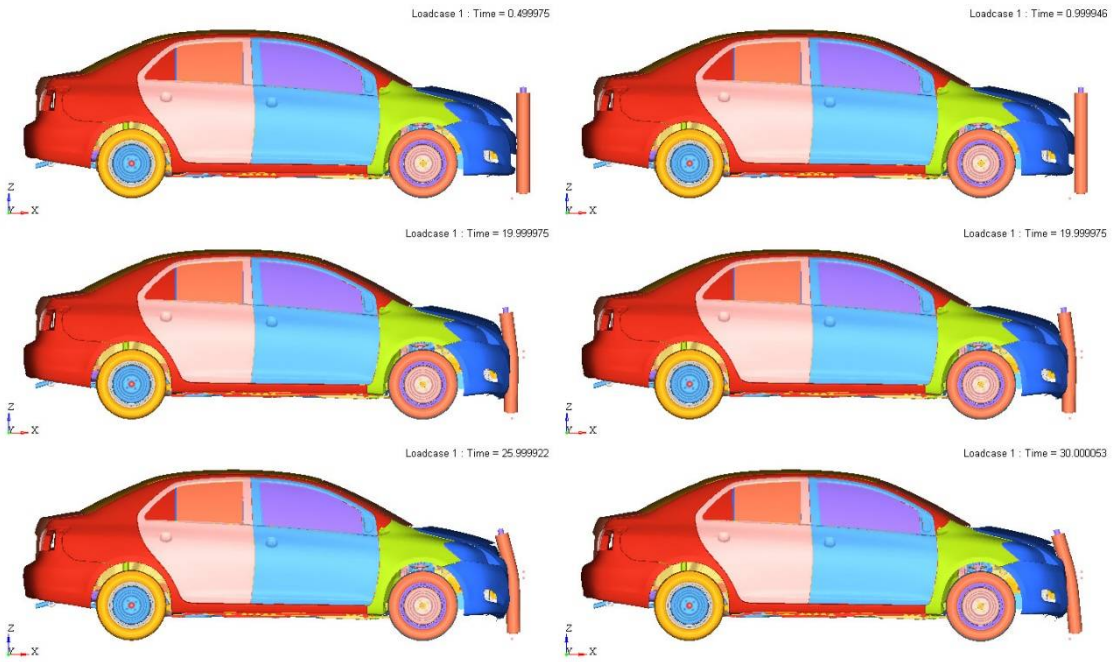

Figure 3.16 Legform collision with Toyota Yaris at 27 kmh

A post and pre simulation of Ford Taurus is depicted in Figure 3.17, as it is performed on lower legform impactor to verify that its performance is within EEVC criteria limit. Since the legform model consist of rigid bodies connected by joints, and finite elements the knee joint is more effect in the whole simulation.

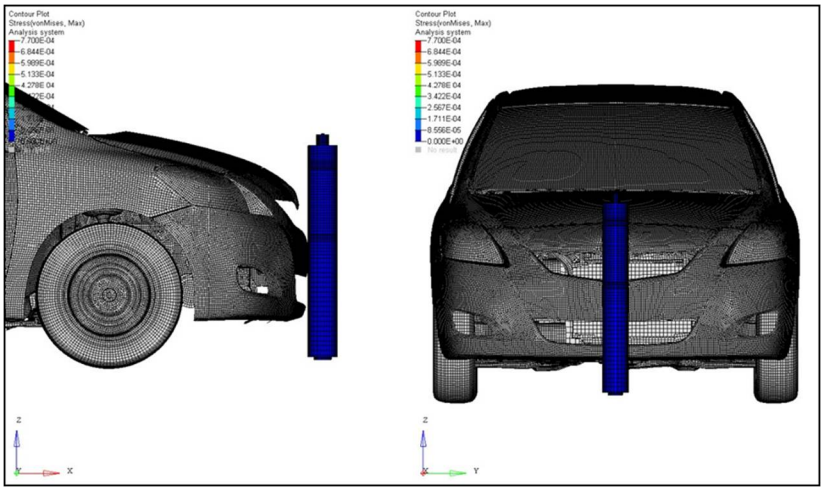

Figure 3.17 Post and pre-simulations of Toyota Yaris

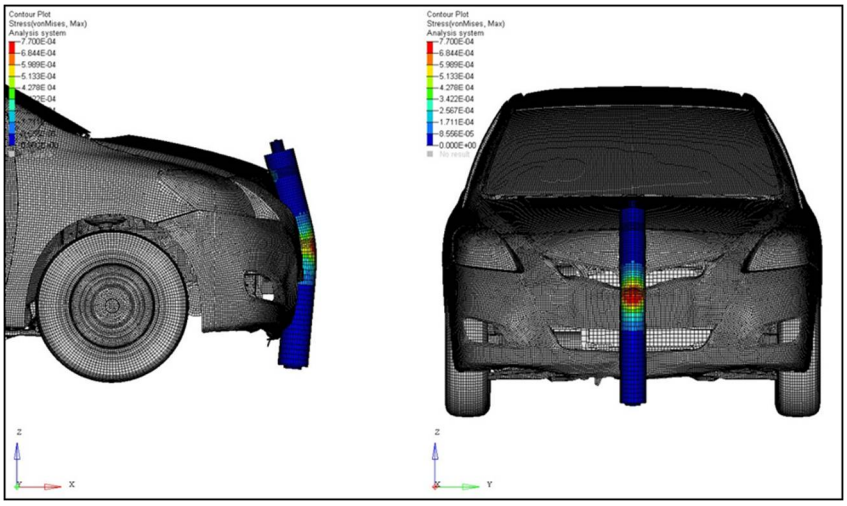

Figure 3.17 (continued)

The knee bending angle in legform impactor when strikes with Toyota Yaris at 27 kmh analyses is shown in Figure 3.16. The maximum knee bending angle in the car model was within the EEVC acceptable criteria and by changing the position, material and increasing the velocity of the impactor, the maximum knee bending angle can also be increased. The maximum bending angle obtained as 7.9 for a run of 30ms. The simulation result in shown in the Figure 3.18.

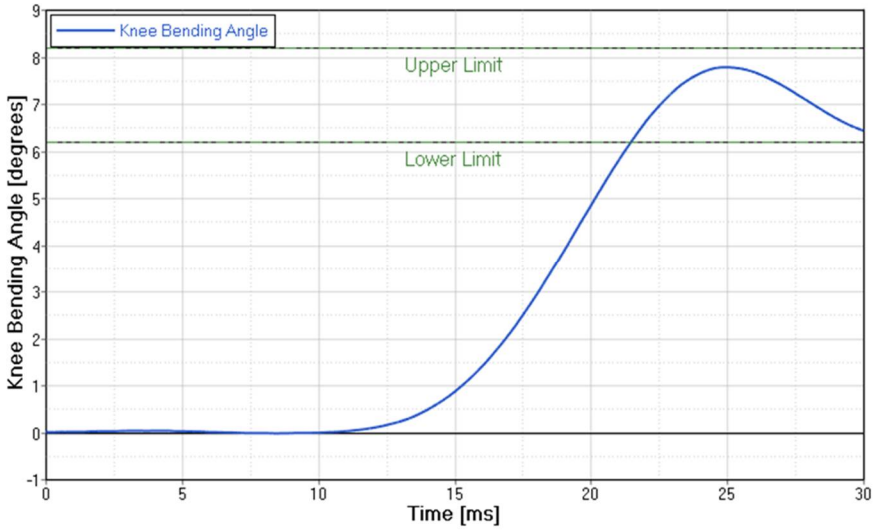

Figure 3.18 Maximum knee bending angle at initial velocity at 27 kmh

The knee shear displacement from the above analyses are shown in Figure 3.19 respectively. The knee shearing displacement was within the EEVC acceptable criteria with displacement done by potentiometer .the knee shearing displacement is corresponds to the bumper design and its stiffness of the material used. The knee shear displacement for the above analyses is obtained as 5.2mm for a run of 30ms.

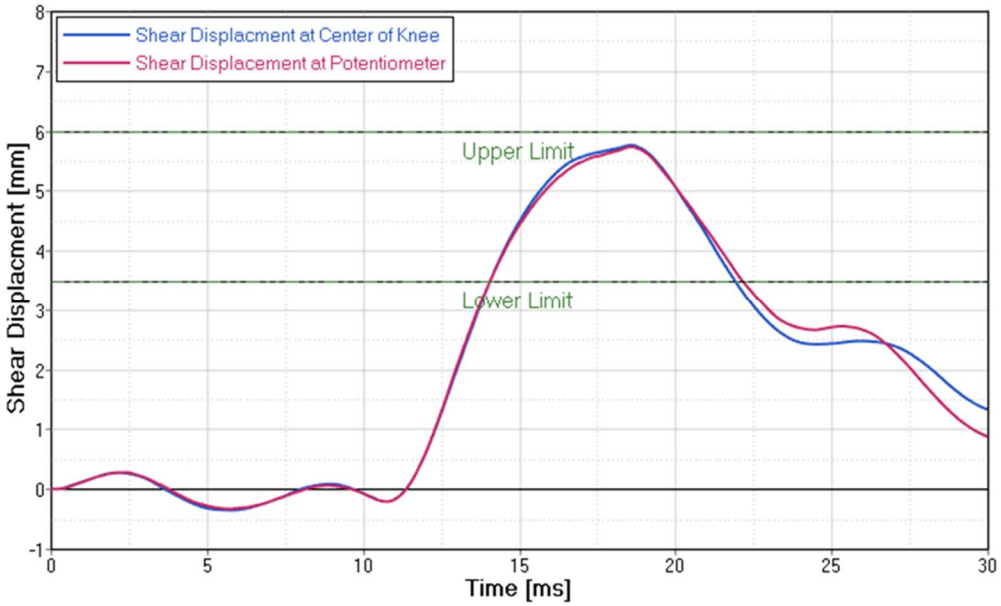

Figure 3.19 Maximum shear displacement at 27 kmh

Tibia acceleration responses is shown in Figure 3.20. The Upper tibia acceleration increases if the strength of the car model is more stable to respond the collision. The tibia acceleration gives the result as soon as the collision occurs with car model. The maximum acceleration obtained for this analyses is 201g for a run of 30ms. When the legform impactor was impacted by high frontal bumper beams, there was higher stiffness properties in the bumper beam material and very little deformation in the bumper assembly, so resulting in upper tibia acceleration increased.

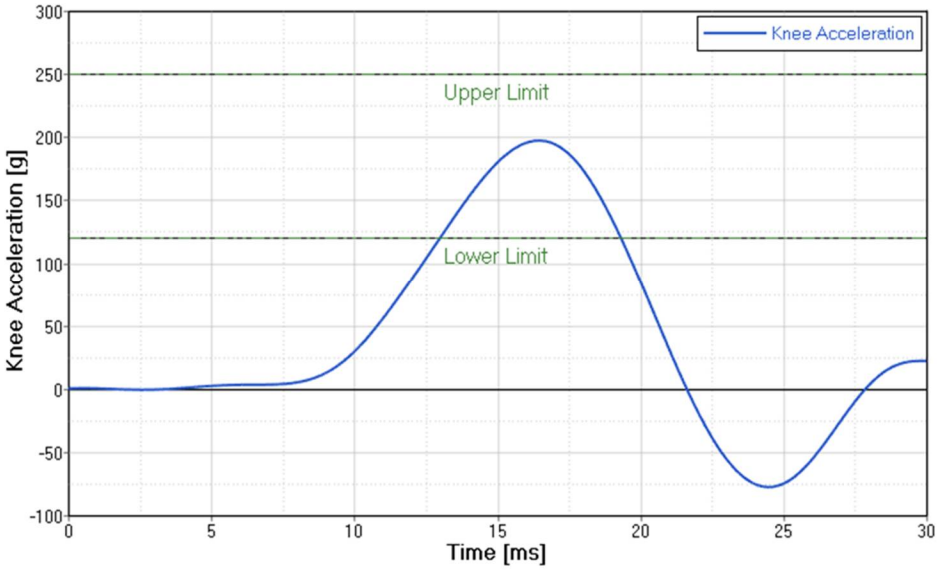

Figure 3.20 Maximum tibia acceleration at initial velocity 27 kmh

3.3.4 Kinematics of FE legform simulation with Toyota Yaris at 40 kmh

The legform-car model impact was imposed at 40 kmh velocity parallel to the longitudinal axis of the vehicle, and initial conditions of analyses were as mentioned in EEVC working group 17. Figure. 3.21 shows the legform-car model collision.

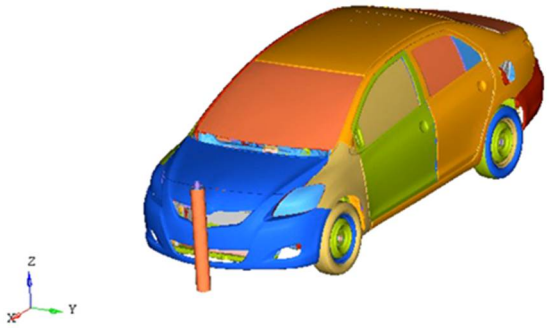

Figure 3.21 Legform impact with car model at 40 kmh

The knee bending angle in legform impactor when strikes with Toyota Yaris model at 40 kmh analyses is shown in Figure 3.22. The maximum knee bending angle in the car model was within the EEVC acceptable criteria and by changing the position, material and increasing the

velocity of the impactor, the maximum knee bending angle can also be increased. The maximum bending angle obtained as 8.0 for a run of 30ms. The simulation result in shown in the Figure 3.23.

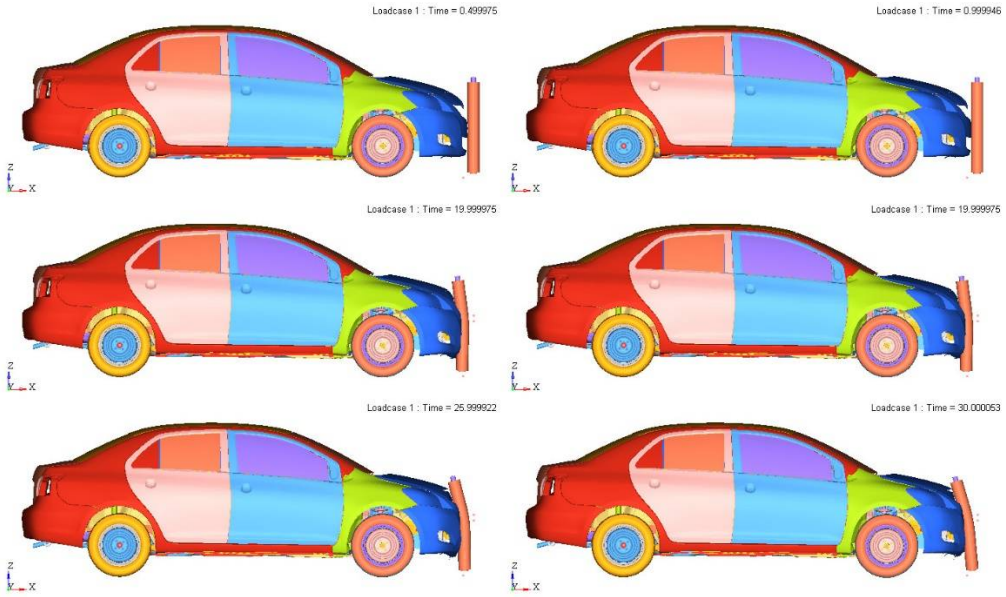

Figure 3.22 Legform collision with Toyota Yaris at 40 kmh

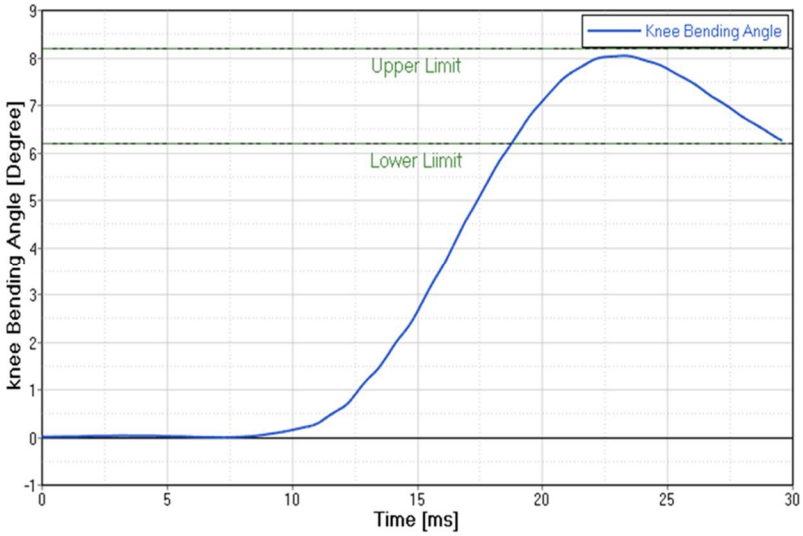

Figure 3.23 Maximum knee bending angle at initial velocity 40 kmh

The knee shear displacement from the above analyses are shown in Figure 3.24 respectively. The knee shearing displacement was within the EEVC acceptable criteria with displacement done by potentiometer .the knee shearing displacement is corresponds to the bumper

design and its stiffness of the material used. The knee shear displacement for the above analyses is obtained as 5.30mm for a run of 30ms

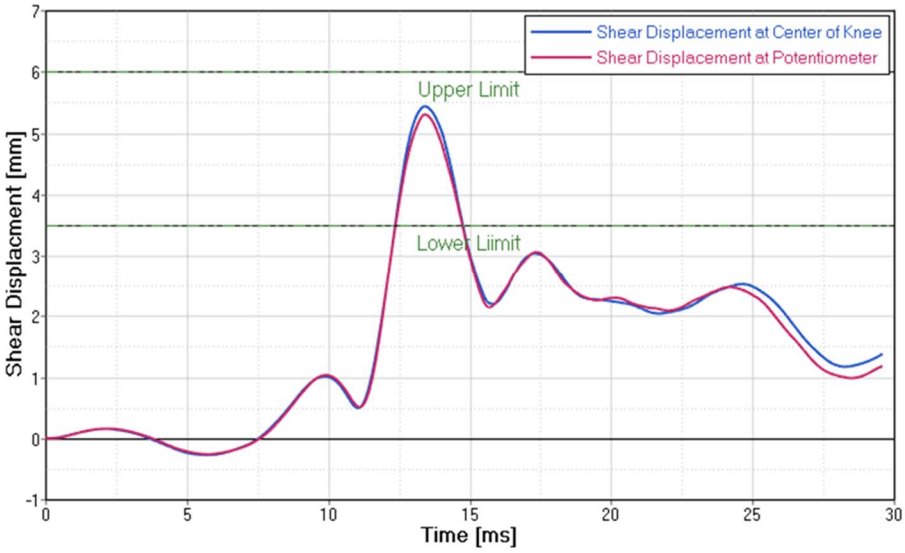

Figure 3.24 Maximum shear displacement at 40 kmh

Tibia acceleration responses is shown in Figure 3.25. The upper tibia acceleration increases if the strength of the car model is more stable to respond the collision .The tibia acceleration gives the result as soon as the collision occurs with car model .the maximum acceleration obtained for this analyses is 202g for a run of 30ms.

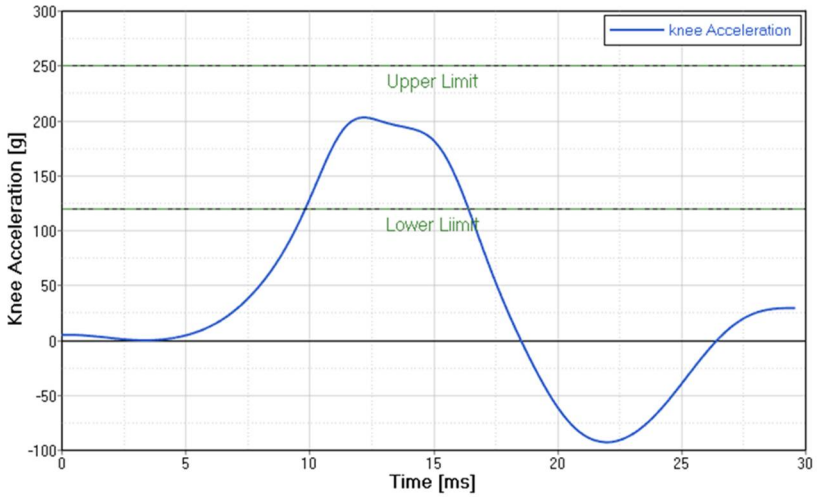

Figure 3.25 Maximum tibia acceleration at initial velocity 40 kmh

CHAPTER 4

ELLIPSIODAL LEGFORM FULL-SIZE PEDSTRIAN AND VEHICLE MODELING AND IMPACT ANALYSIS

4.1 Legform Ellipsoidal Model in MADYMO

The basis of the legform models is formed by a chain of three rigid bodies. These bodies represent respectively the femur steel and foam, (part of) the shear spring and the tibia steel and foam. The bodies Femur_bod and ShearSpring_bod are connected with a translational joint (ShearSpring_jnt) to represent the shear displacement in shear spring. The bodies ShearSpring_bod and Tibia_bod are connected with a revolute joint (Knee_jnt) that represents the deformable knee ligaments.A simple Ellipsoidal Model Shown in Figure 4.1 [29].

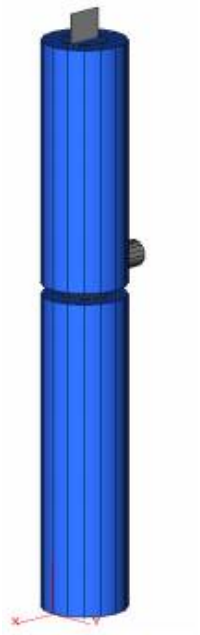

Figure 4.1 Ellipsoidal legform model

A joint restraint on the shear spring translational joint is used to model the shear spring stiffness and the end stops for the shear displacements when steel-to-steel contact occurs between shear spring end and inner femur tube. The effect of the damper is included in this joint restraint

model with a constant damping coefficient. A second joint restraint, working on the knee revolute joint, is included to model the bending stiffness of the knee ligaments. Hysteresis is included in the loading characteristic in order to model the plasticity of the ligament deformation. Both the shear spring and the knee bending characteristic are directly derived from the static legform certification corridors as defined by EEVC-WG17. The force-deflection curves correspond to loading curves in the middle of the static shear and bending certification corridors. A point restraint between Femur_bod and Tibia_bod is included to represent flesh and skin influence on the shear behaviour [29].

The outer legform surface is represented by two separate cylinders: one for the femur and one for the tibia region. The foam and skin compliance is lumped in a predefined force-based contact characteristic that includes hysteresis. For simulations in which the bumper system is modelled with ellipsoids, hysteresis of the bumper ellipsoids can be modelled with any hysteresis model as long as the loading and unloading curve are strictly increasing and include zero force for zero penetration. The characteristics of the legform and bumper can then be combined using CONTACT_FORCE_CHAR with CONTACT_TYPE = COMBINED. Purely for visualisation, the damper assembly on the back- or non-impact side of the legform impactor is also represented with a cylinder. The ellipsoid legform model geometry as well as the rigid body inertia properties are defined such that all the EEVC-WG17 design specifications are met. The ShearSpring joint displacements and the Knee joint deflection angle are used as output to represent the measured legform knee shear displacement and knee bending angle. The tibia acceleration measurement is represented by linerar acceleration output at the appropriate location on the tibia body [29].

4.2 Vehicle Ellipsoidal Model Development

Madymo utilizes both Multibody analysis, which simulates the gross motion of system of bodies connected by complicated joints, and finite element techniques, used for simulation of structural behavior.

The finite element divides the actual continuum into finite volumes, surfaces or line segments. Each element deforms according to specified load-deformation relationship. The continuum is then analyzed as complex system, composed of relatively simple elements where continuity is ensured along all boundaries between elements. These elements are interconnected at a discrete number points or nodes. The data required for the simulation include initial nodal positions and velocities, the nodes corresponding to each element

The vehicle model shown in Figure 4.2 is developed which represents a similar geometry compared to FE model used, but with less components to the frontal side and making one body system, planes and ellipses are connected to each other to make the vehicle geometry. The seat and floor are modelled by rigid and they are connected to vehicle system. In this car model the velocity performed are at 27kmph, and 40kmph respectively. The moment of inertia is about X-axis corresponding to the center of gravity .the equivalent stiffness of the vehicle ellipsoidal design car is given in Figure 4.2. The load-deformation characteristic curves is assumed to be same when modelling the car crash with pedestrian model and legform impactor.

The description of design model of car model gives specification of the bumper Centre height as 509mm. The Windshield length as 820mm with center of gravity acting in middle of the car. The speed is defined by initial joint velocity and overall weight of the car corresponds to the FE model.

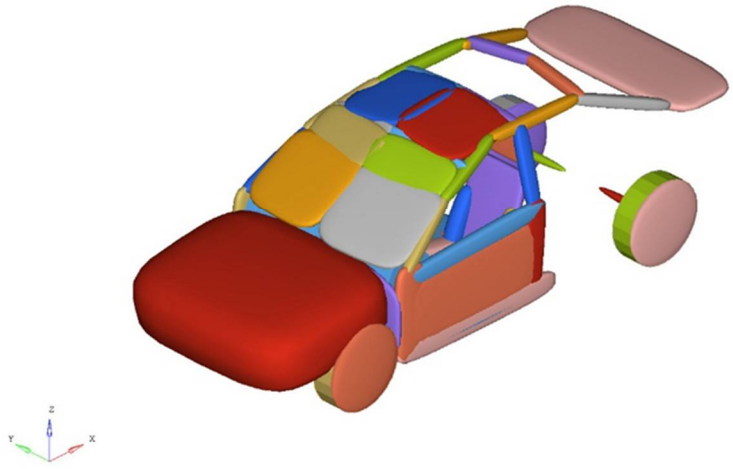

Figure 4.2 Ellipsoidal car model

4.3 Ellipsoidal Legform and Vehicle Impacts

4.3.1 Kinematics of ellipsoidal legform simulation with ellipsoidal car model at 27 kmh

The Ellipsoidal legform-ellipsoidal car model impact was imposed at 27 kmh velocity parallel to the longitudinal axis of the vehicle, and initial conditions of analyses were as mentioned in EEVC Working Group 17. Figure 4.3 shows the ellipsoidal legform-car model collision.

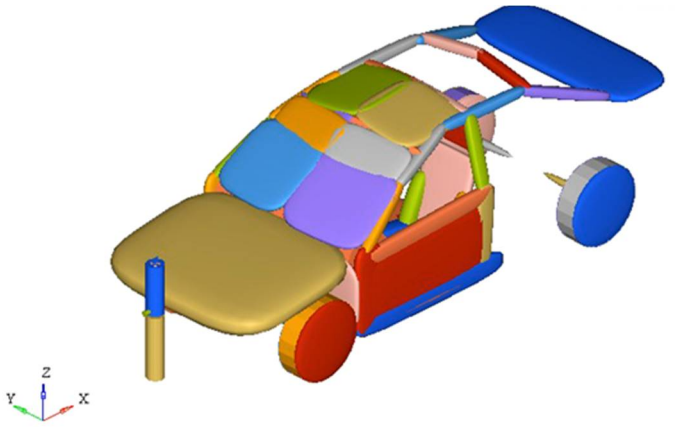

Figure 4.3 Legform Impact with car model at 27 kmh

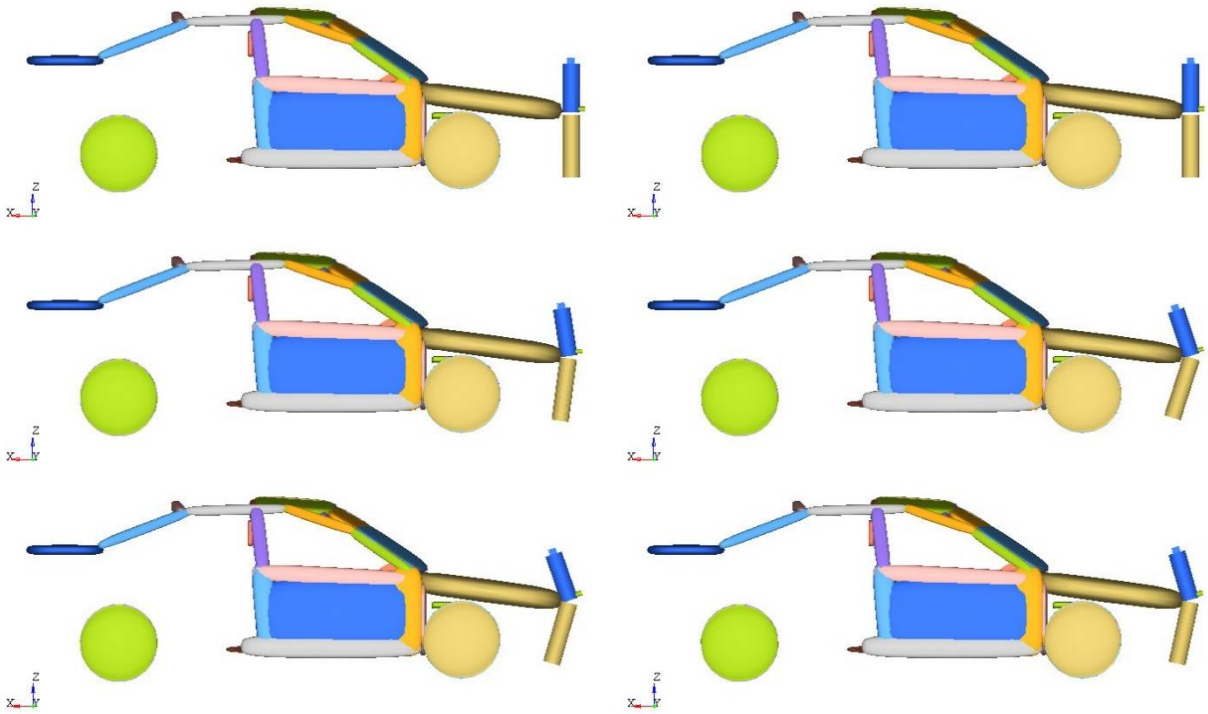

Figure 4.4 Legform collision with ellipsoidal car model at 27 kmh

The knee bending angle in legform impactor when striken with the ellipsoidal car model at 27 kmh analysis is shown in Figure 4.4.

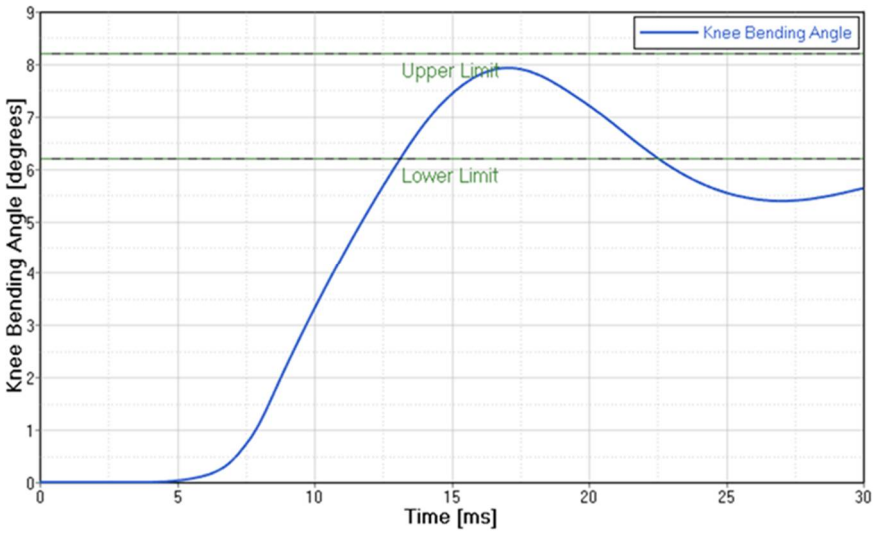

Figure 4.5 Maximum knee bending angle at initial velocity 27 kmh

The maximum knee bending angle in the car model was within the EEVC acceptable criteria and by changing the position, material and increasing the velocity of the impactor, the maximum knee bending angle can also be increased. The maximum bending angle obtained as 7.9 for a run of 30ms. The simulation result in shown in Figure 4.5.

The knee shear displacement from the above analyses are shown in Figure 4.6 respectively. The knee shearing displacement is corresponds to the bumper design and its stiffness of the material used. The knee shear displacement for the above analyses is obtained as 4.90mm for a run of 30ms.

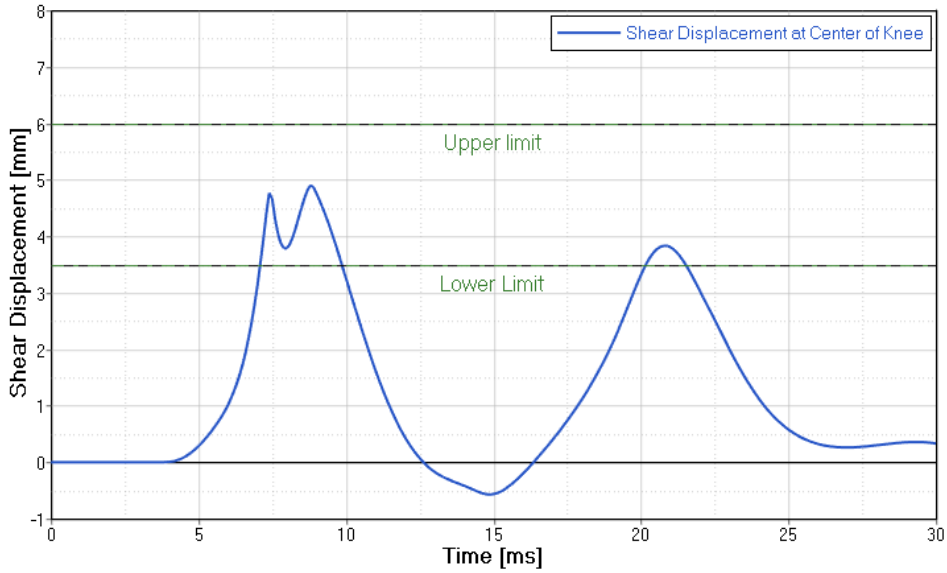

Figure 4.6 Maximum shear displacement at 27 kmh

Tibia acceleration responses is shown in Figure 4.7. The Upper Tibia Acceleration increases if the strength of the car model is more stable to respond the collision .the tibia acceleration gives the result as soon as the collision occurs with car model .the maximum acceleration obtained for this analyses is 193g for a run of 30ms.

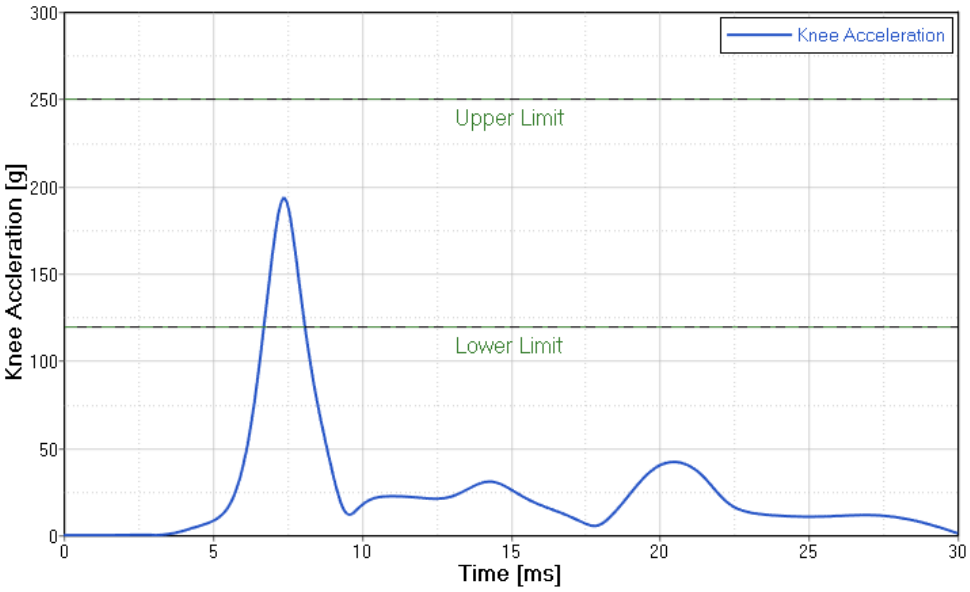

Figure 4.7 Maximum tibia acceleration at initial velocity 27 kmh

4.3.2 Kinematics of ellipsoidal legform simulation with ellipsoidal car model at 40 kmh

The Ellipsoidal legform-ellipsoidal car model impact was imposed at 40 kmh velocity parallel to the longitudinal axis of the vehicle, and initial conditions of analyses were as mentioned in EEVC Working Group 17 Figure 4.8 shows the ellipsoidal legform-car model collision.

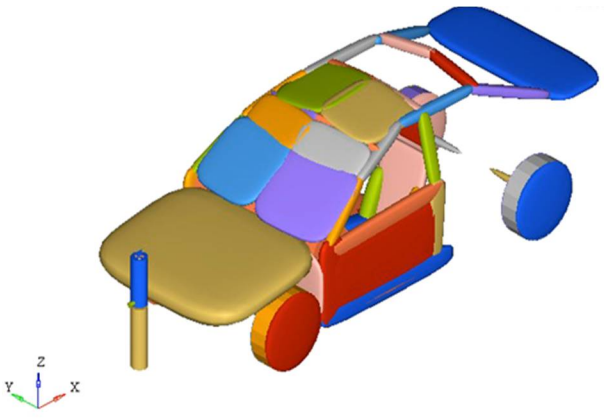

Figure 4.8 Legform impact with car model at 40 kmh

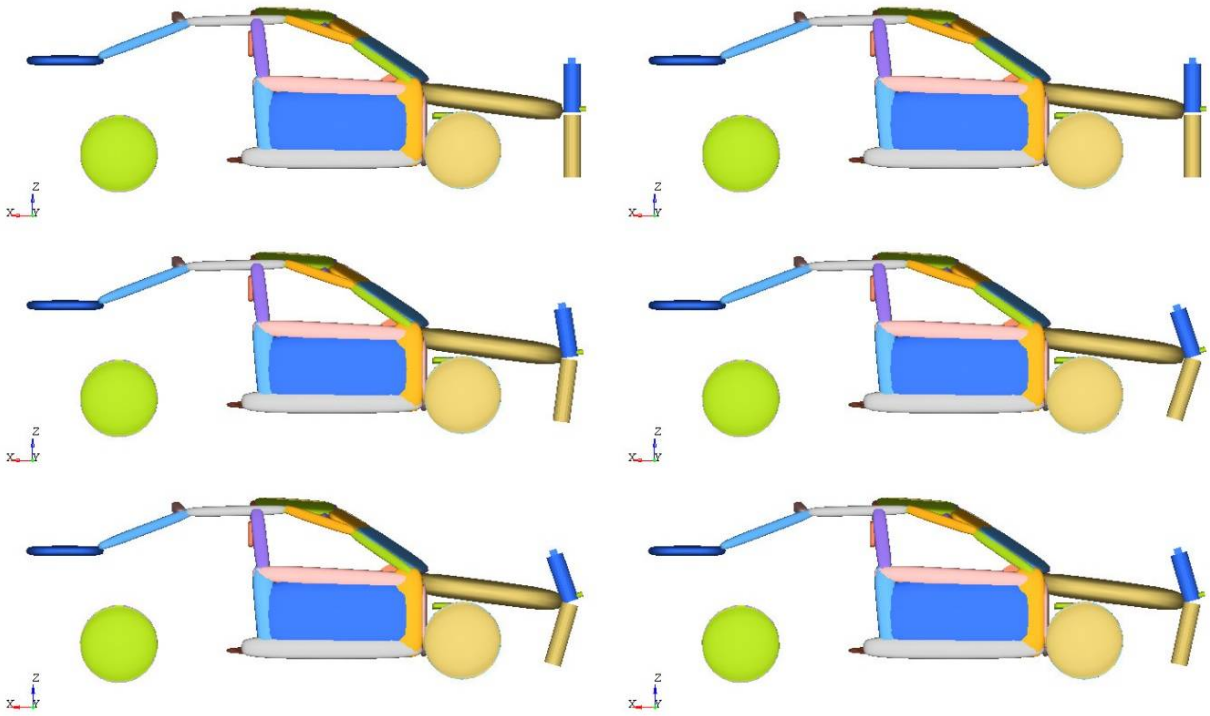

Figure 4.9 Legform collision with ellipsoidal car model at 40 kmh

The knee bending angle in legform impactor when impacted with ellipsoidal car model at 40 kmh analysis is shown in Figure 4.9.

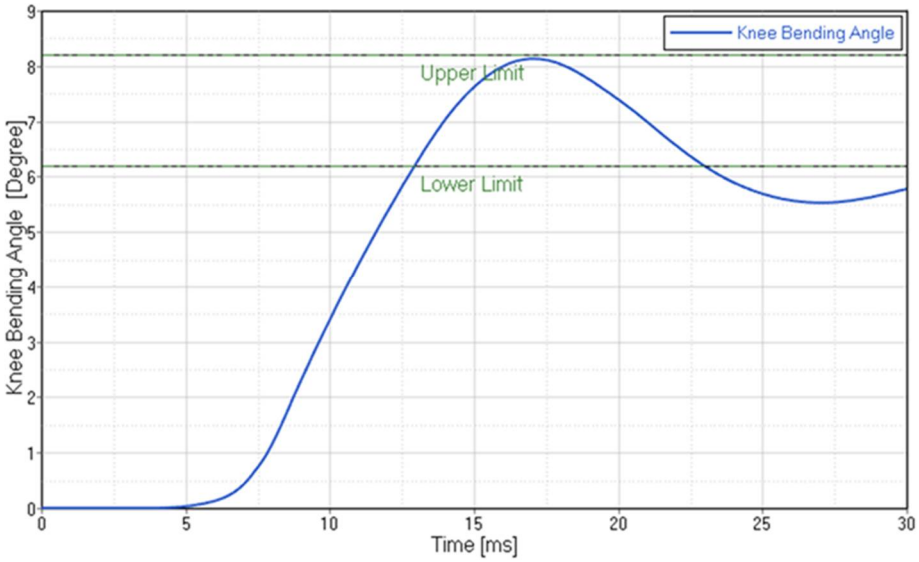

Figure 4.10 Maximum knee bending angle at initial velocity 27 kmh

The maximum knee bending angle in the car model was within the EEVC acceptable criteria and by changing the position, material and increasing the velocity of the impactor, the maximum knee bending angle can also be increased. The maximum bending angle obtained as 8.1 for a run of 30ms. The simulation result shown in the Figure 4.10.

The knee shear displacement from the above analyses are shown in Figure 4.11 respectively. The knee shearing displacement was within the EEVC acceptable criteria with displacement done by potentiometer .the knee shearing displacement is corresponds to the bumper design and its stiffness of the material used. The knee shear displacement for the above analyses is obtained as 5.5mm for a run of 30ms.

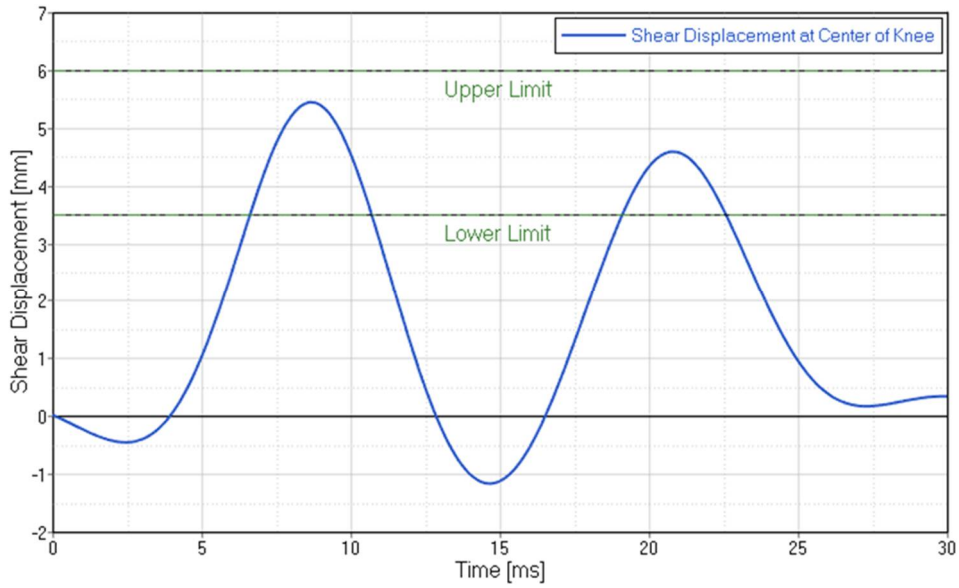

Figure 4.11 Maximum shear displacement at 27 kmh

Tibia acceleration responses is shown in Figure 4.12. The upper tibia acceleration increases if the strength of the car model is more stable to respond the collision .the tibia acceleration gives the result as soon as the collision occurs with car model .the maximum acceleration obtained for this analyses is 198g for a run of 30ms.

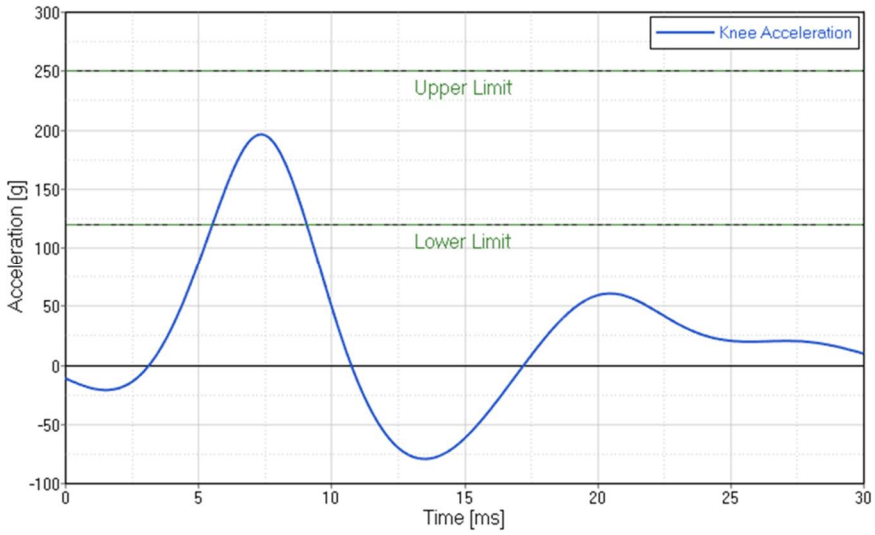

Figure 4.12 Maximum tibia acceleration at initial velocity 27 kmh

4.4 Pedestrian Model and Ellipsoidal Car Impact Simulation

4.4.1 Kinematics of pedestrian model simulation with ellipsoidal car model at 27 kmh

The pedestrian model-ellipsoidal car model impact was related at 27 kmh velocity parallel to the longitudinal axis of the vehicle, and initial conditions of analyses were as mentioned in EEVC Working Group 17. Figure 4.13 shows the legform-car model collision kinematics.

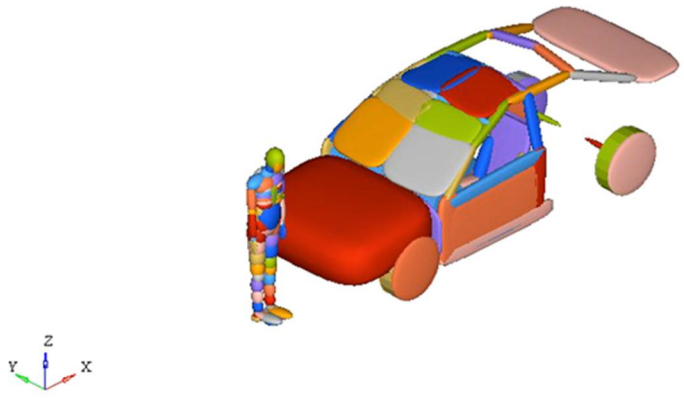

Figure 4.13 Legform impact with car model at 27 kmh

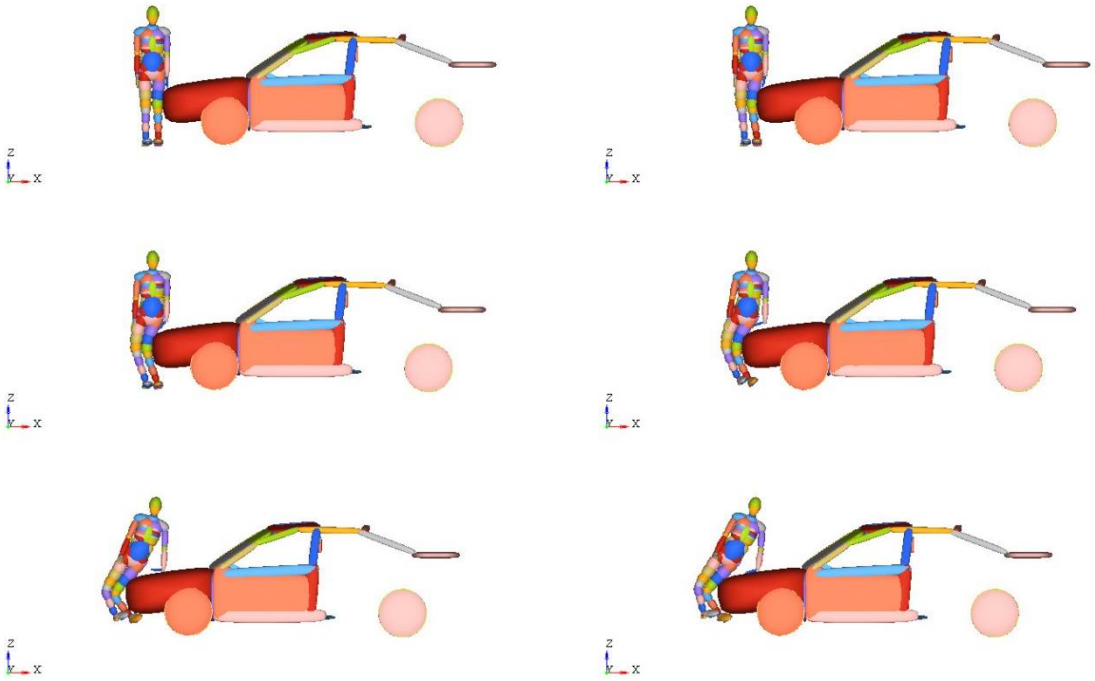

Figure 4.14 Pedestrian model collision with ellipsoidal car

The knee bending angle in legform impactor when strikes with pedestrian model at 27 kmh analysis is shown in Figure 4.14.

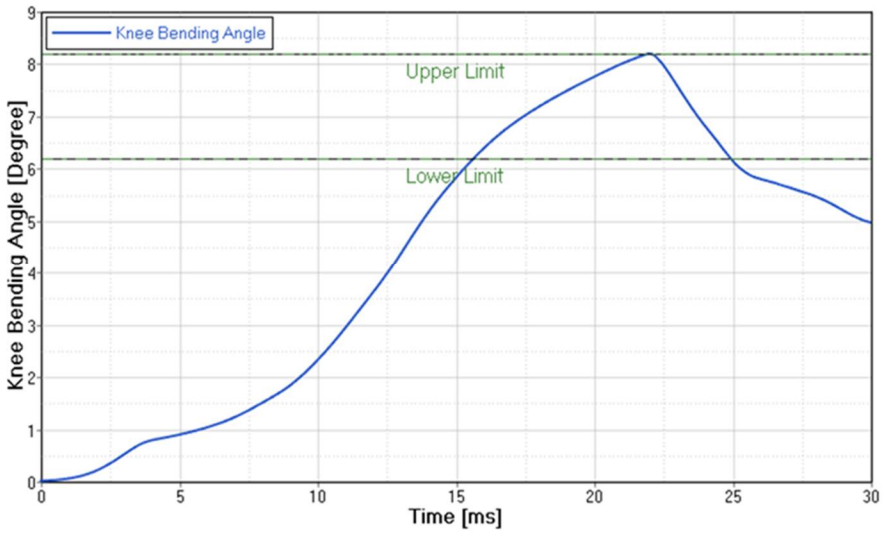

Figure 4.15 Maximum knee bending angle at initial velocity 27 kmh

The maximum knee bending angle in the car model was within the EEVC acceptable criteria and by changing the position, material and increasing the velocity of the impactor, the maximum knee bending angle can also be increased. The maximum bending angle obtained as 8.2 for a run of 30ms. The simulation result in shown in Figure 4.15.

The knee shear displacement from the above analyses are shown in Figure 4.16 respectively. The knee shearing displacement was within the EEVC acceptable criteria with displacement done by potentiometer .the knee shearing displacement is corresponds to the bumper design and its stiffness of the material used. The knee shear displacement for the above analyses is obtained as 5.90mm for a run of 30ms.

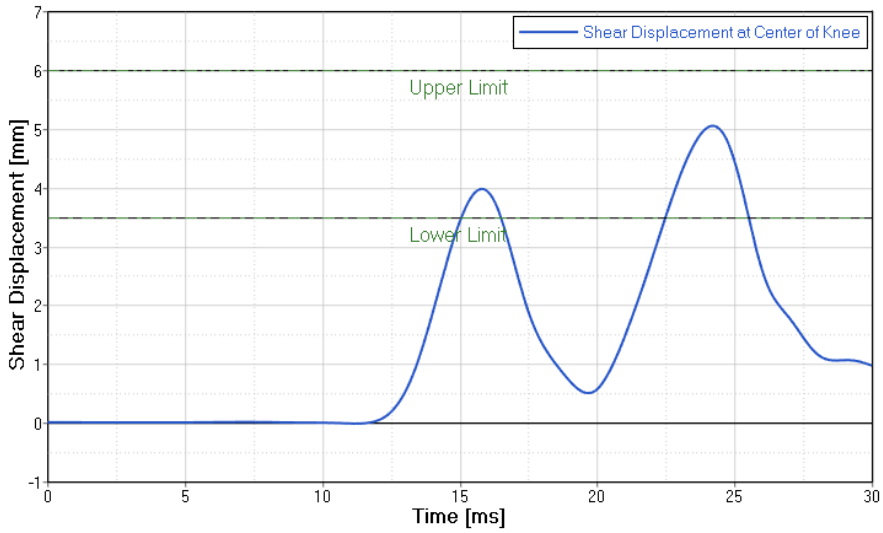

Figure 4.16 Maximum shear displacement at 27 kmh

Tibia acceleration respones is shown in Figure 4.17. The upper tibia acceleration increases if the strength of the car model is more stable to respond the collision .the tibia acceleration gives the result as soon as the collision occurs with car model .the maximum acceleration obtained for this analyses is 217g for a run of 30ms.

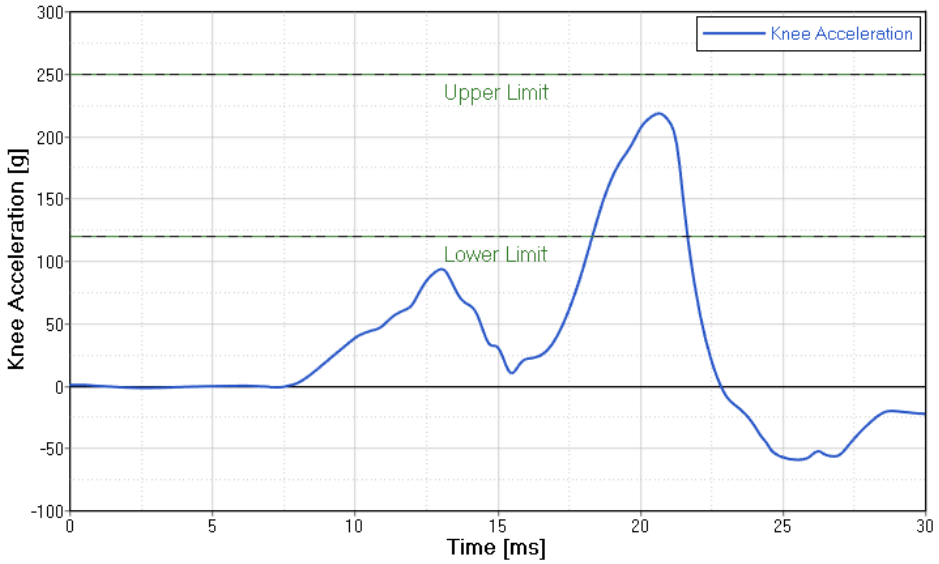

Figure 4.17 Maximum tibia acceleration at initial velocity 27 kmh

4.4.2 Kinematics of pedestrian model simulation with ellipsoidal car model at 40 kmh

The pedestrian model-ellipsoidal car model impact was simulated at 40 kmh velocity parallel to the longitudinal axis of the vehicle, and initial conditions of analyses were as mentioned in EEVC Working Group 17. Figure 4.18 shows the legform-car model collision.

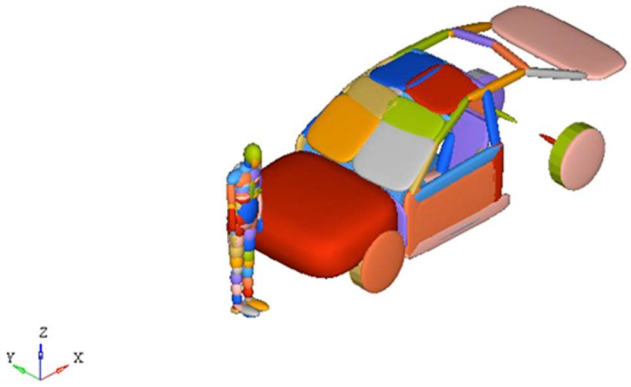

Figure 4.18 Legform impact with car model at 40 kmh

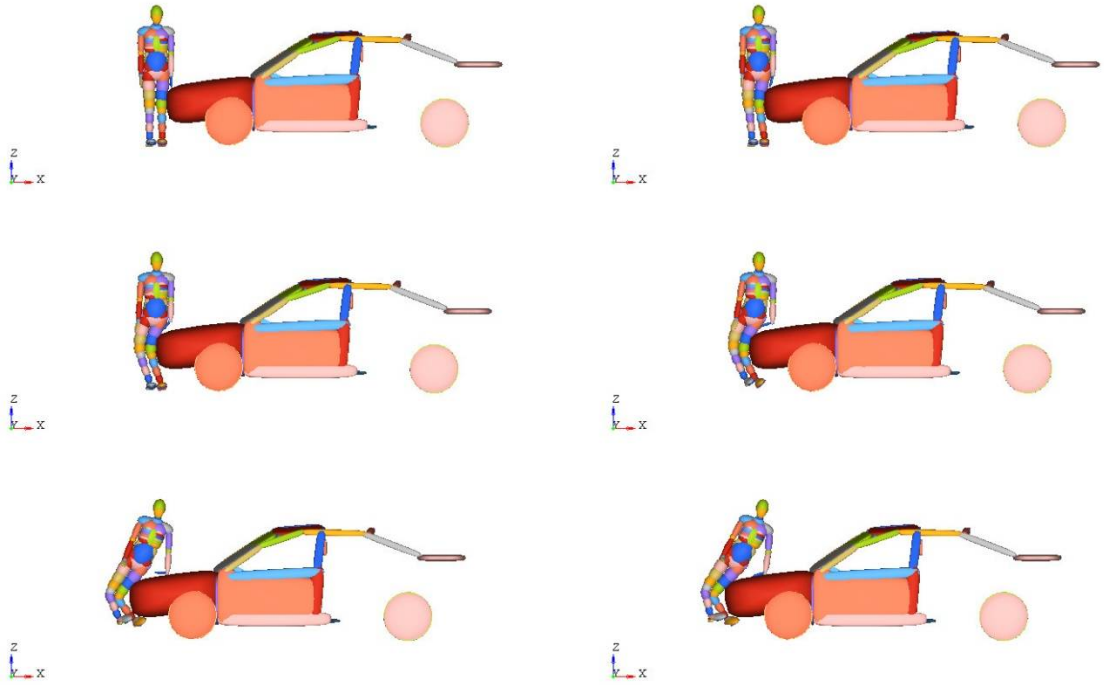

Figure 4.19 Pedestrian model collision with ellipsoidal car

The knee bending angle in legform impactor when strikes with Toyota Yaris model at 40 kmh analyses is shown in Figure. 4.19.

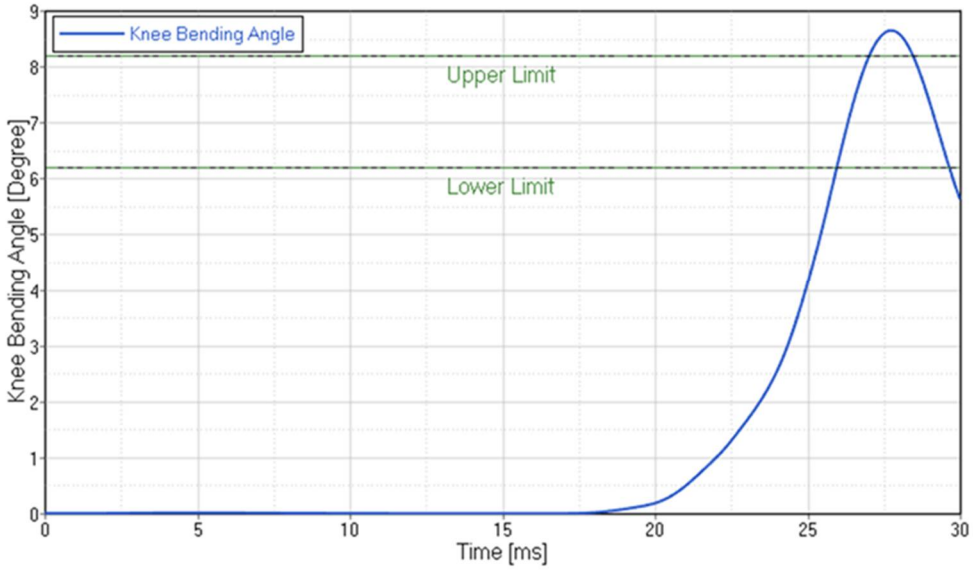

Figure 4.20 Maximum knee bending angle at initial velocity 40 kmh

The maximum knee bending angle in the car model was within the EEVC acceptable criteria and by changing the position, material and increasing the velocity of the impactor, the maximum knee bending angle can also be increased. The maximum bending angle obtained as 8.8 for a run of 30ms. The simulation results are shown in Figure 4.20.

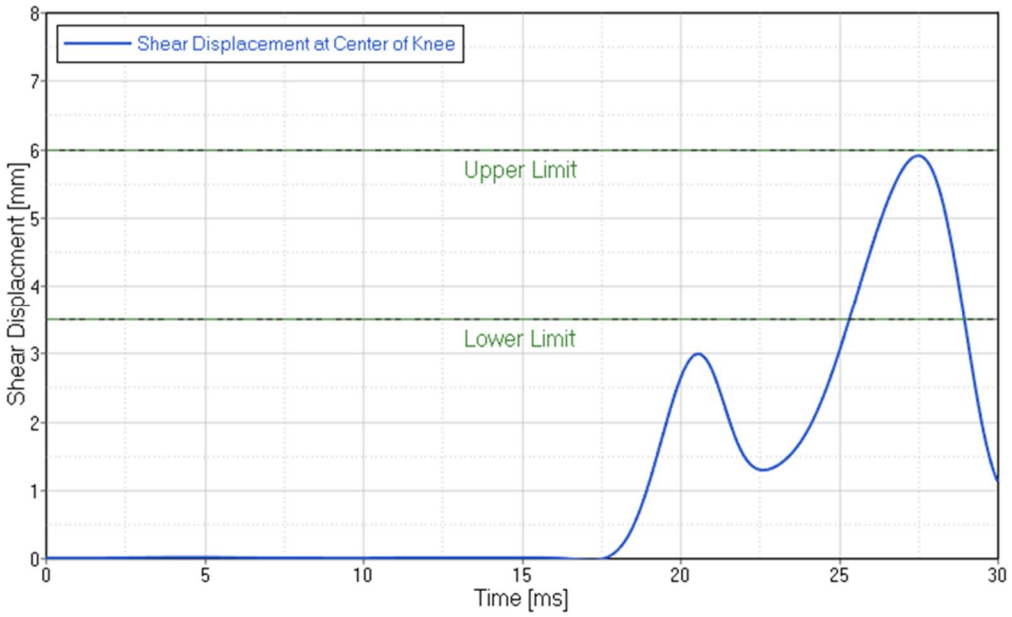

Figure 4.21 Maximum shear displacement at 40 kmh

The knee shear displacement from the above analyses are shown in Figure 4.21 respectively. The knee shearing displacement was within the EEVC acceptable criteria with displacement done by potentiometer .the knee shearing displacement is corresponds to the bumper design and its stiffness of the material used. The knee shear displacement for the above analyses is obtained as 5.0mm for a run of 30ms. By changing the frontal design of higher strength, the initial relative motion of the femur and tibia is changed. This is because with high strength frontal materials, the frontal offers more resistance against the free motion of the femur, and therefore the movement of the tibia in the direction of the collision is higher than that of the femur.

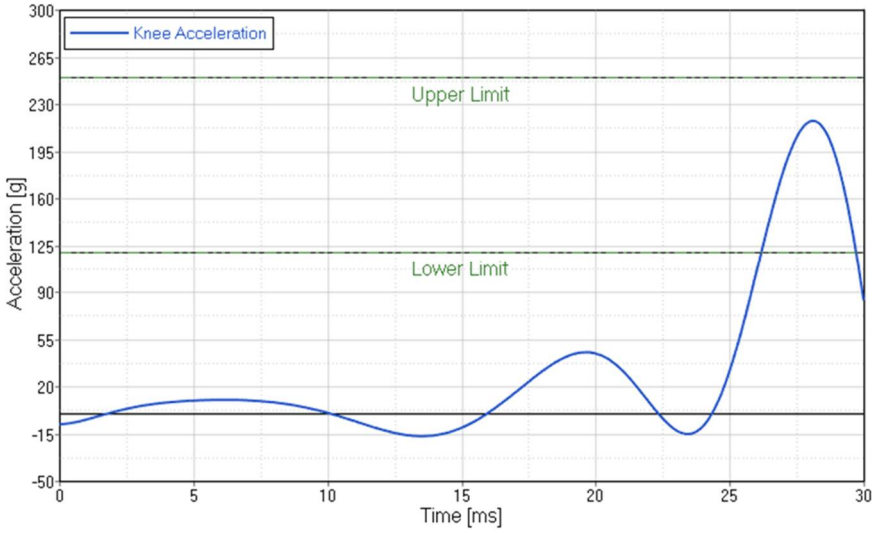

Figure 4.22 Maximum tibia acceleration at initial velocity 40 kmh

Tibia acceleration responses is shown in Figure 4.22. The upper tibia acceleration increases if the strength of the car model is more stable to respond the collision. The tibia acceleration occurs the result as soon as the collision occurs with car model .The maximum acceleration obtained for this analyses was 210g for a run of 30ms.

CHAPTER 5

SUMMARY OF RESULTS AND DISCUSSION

5.1 FE Legform Model versus Ellipsoidal Legform Model

The presented approaches were simulated on different workbenches to assess whether the subsystem lower test matches the criteria proposed by EEVC. The simulation of the Ellipsoidal Legform and Fe Legform are similar in kinematic response which is shown in Figures 5.1 and 5.2 respectively.

The assumption made by multibody legform model are correspond to more close to the pedestrian kinematics. The main frontal side of car model in both cases are crucial to match with actual geometry .thus comparison can be made with the experience and kinematic response of the legform in the both workbenches.

The FE model has the same basic structure as the ellipsoid model. Two ellipsoid cylinders form the femur and tibia. Both are connected by a deformable knee. The difference is that in the FE model the foam layers are modeled by a hollow cylinder consisting of finite elements. This cylinder cover both femur and tibia. In the FE model the influence of the foam does not have to be compensated in other parts of the model.

The mass properties consist of a ellipsoid part (Ellipsoidal) and a FE part. The combined properties (Total) are compared with the prescribed properties. The moments of inertia are calculated around the C.G. of the corresponding body. All products of inertia are zero in this coordinate system.

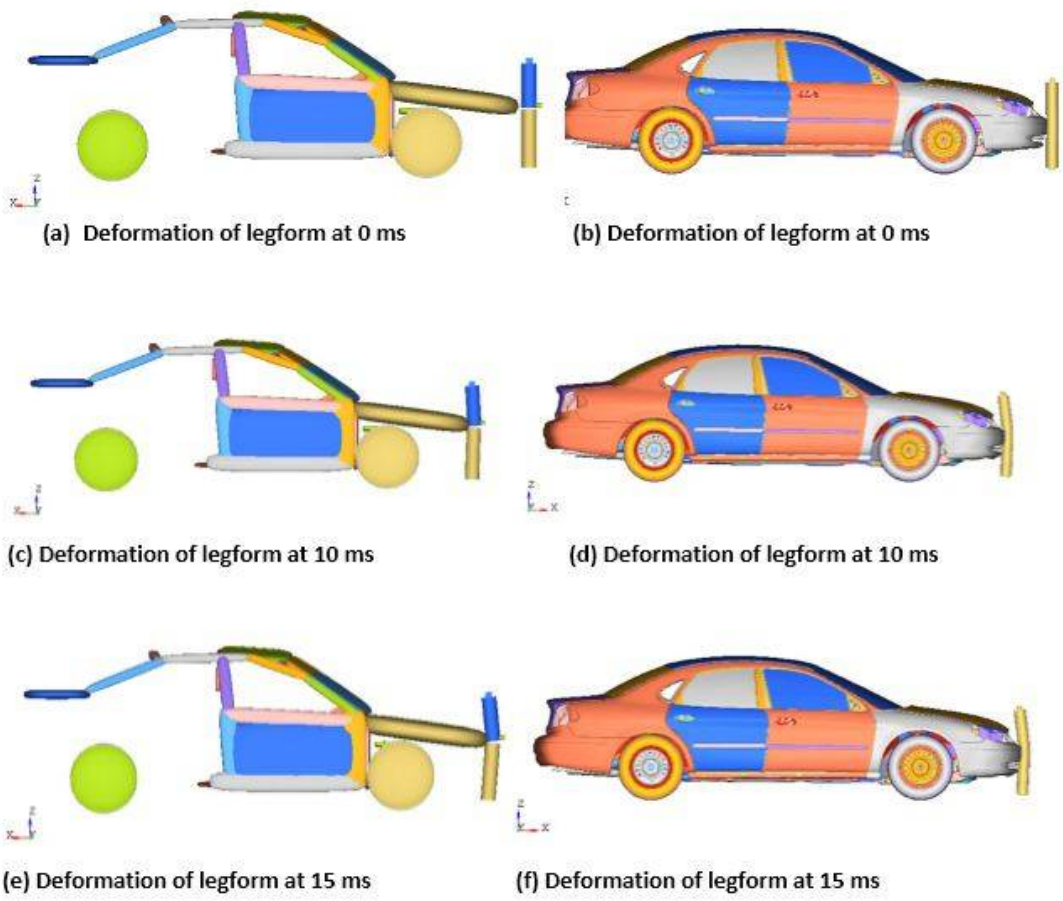

Figure 5.1 Comparison of kinematics of FE subsystem legform and MADYMO legform subsystem

In the analyses performed with FE legform and ellipsoidal legform, the displacement of the legform is corresponded with the velocity impacted towards the car and however the maximum knee bending angle for FE legform occurred at 9−12 ms after collision where as for the ellipsoidal legroom the bending angle is more as compared with FE legform.

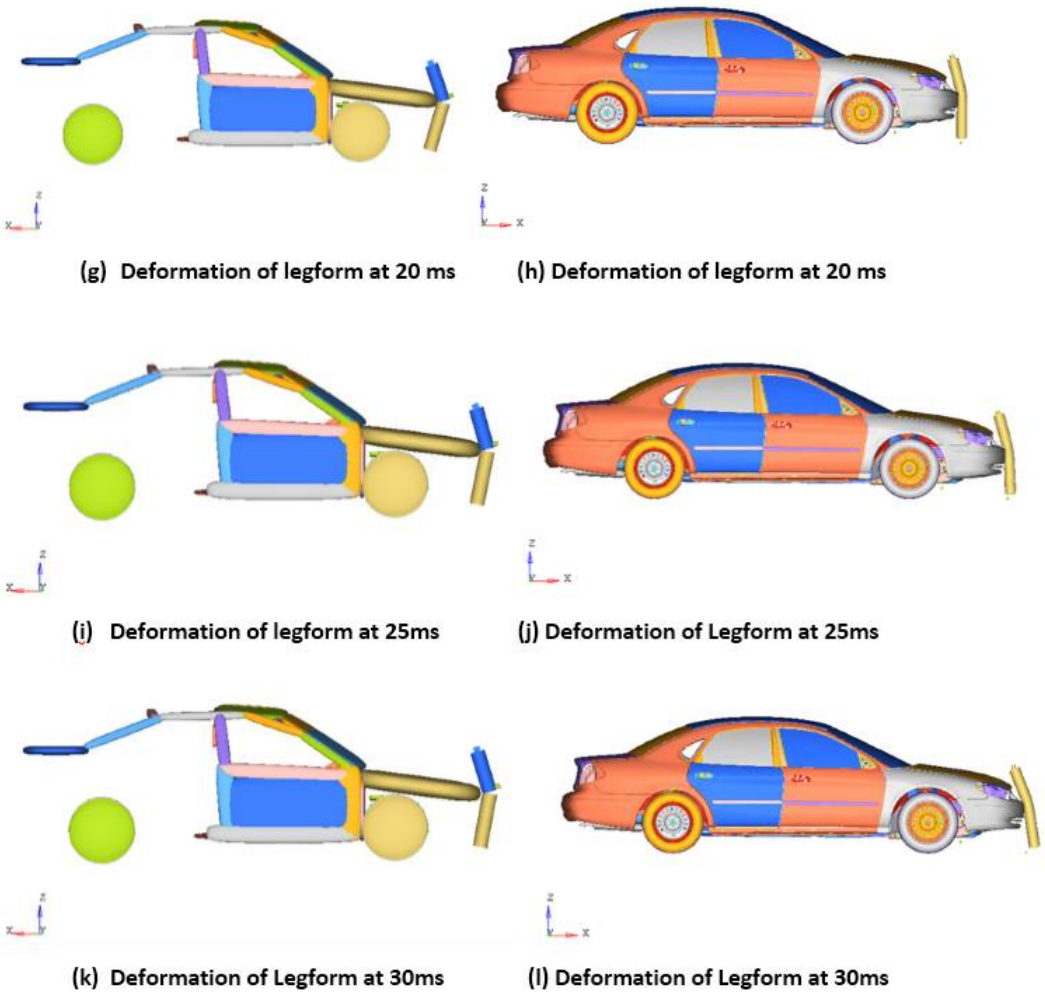

Figure 5.2 Comparison of kinematics of FE subsystem legform and MADYMO legform subsystem

5.2 Full-Size Pedestrian Model versus Legform Model

The comparison done with Pedestrian Male model with two different legform and its kinematics responses are shown in Figure 5.3 and 5.4 respectively. The part of knee bending angle is higher in dummy model as compared to legform models, its estimate that the risk of knee ligament injuries during collision with car model is not absolute for the subsystem used in FE or Ellipsoidal form.

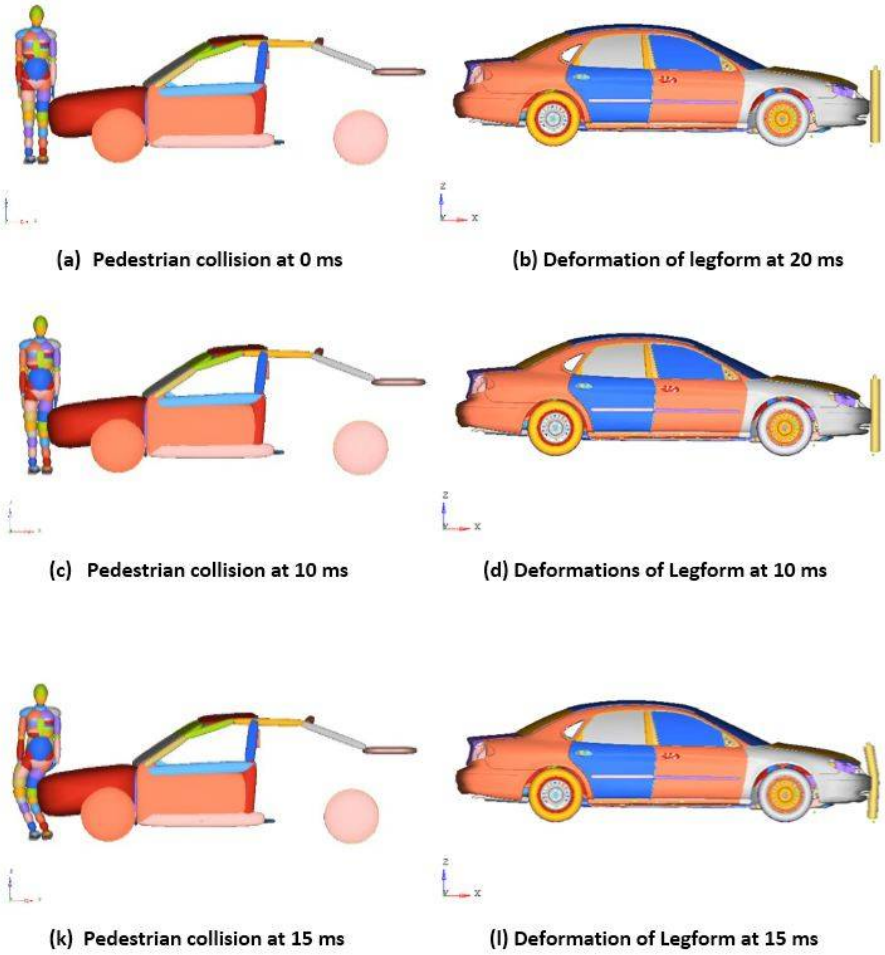

Figure 5.3 Comparison of kinematics of FE subsystem legform and full-size pedestrian models

In the analyses performed with FE legform and full size pedestrian model, the displacement of the legform is corresponded with the velocity impacted towards the car and however the maximum knee bending angle for FE legform occurred at 9−12 ms after collision where as for the FE legform the knee bending angle is higher as compared with FE legform.

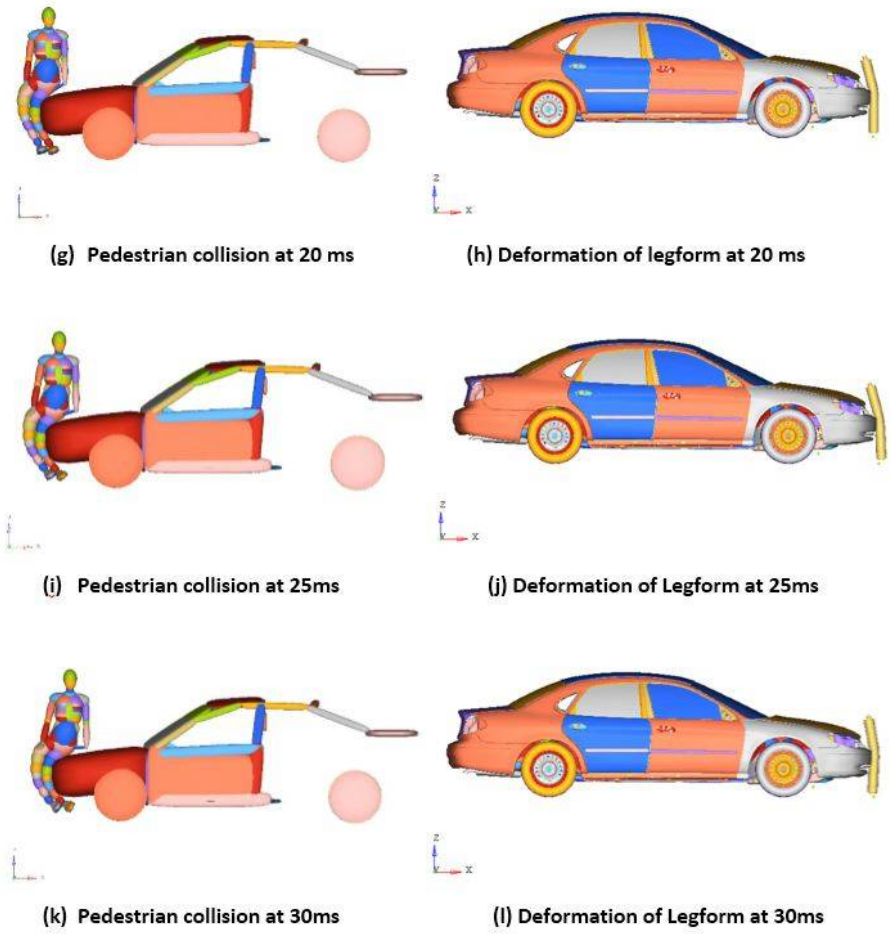

Figure 5.4 Comparison of kinematics of FE subsystem legform and full-size pedestrian models

5.3 Overall Comparison of Simulation Results

5.3.1 Knee bending angle comparison

The knee bending angles for these different speed are shown in Figure 5.5. The knee shearing displacement was within the EEVC acceptable criterion in all analyses and this parameter is not critical for this car model. By using different car model of higher strength, the initial relative motion of the femur and tibia is changed. This is because with high strength frontal material used by manufactures, the frontal side is higher in strength for these car models and therefore the movement of the tibia in the direction of the collision is greater than that of the femur.

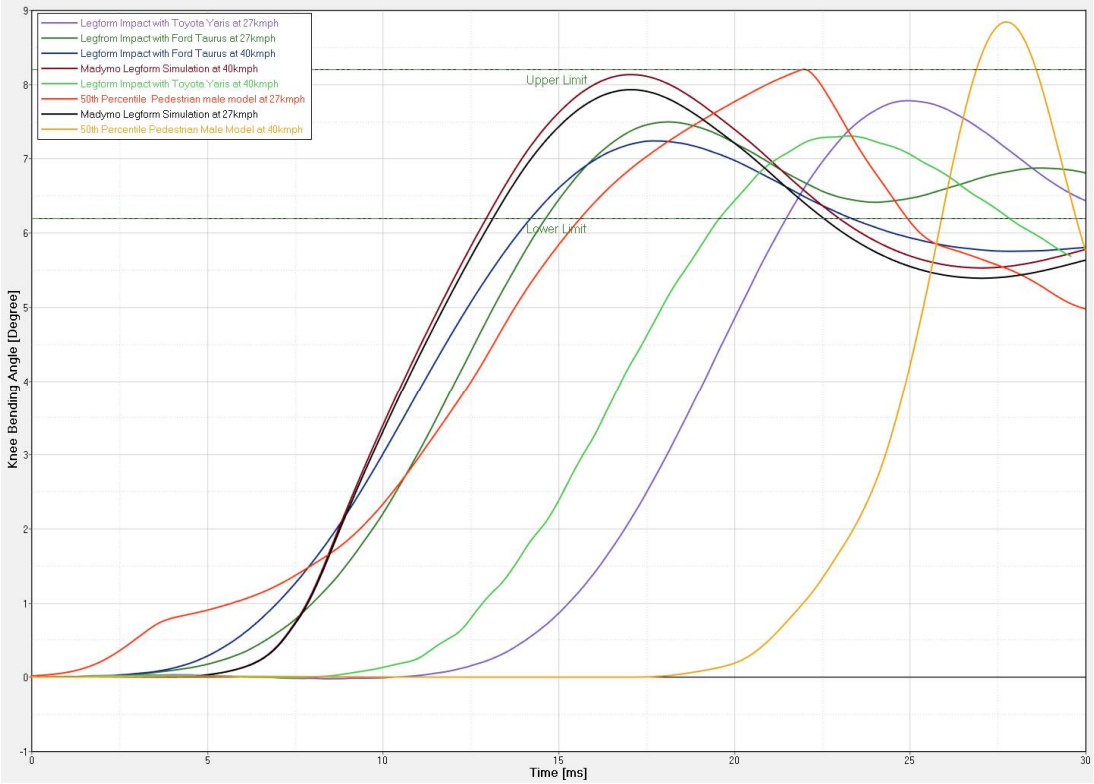

Figure 5.5 Comparision of knee bending angle with legform and full size pedestrian

A brief comparison is shown in the Table 5.1, where the legform impactor with FE car model and MADYMO ellipsoidal model variation with changes in bending angle at different speed respectively. The following results concluded by the FE legform model and ellipsoidal legform with full size pedestrian are

- The maximum knee bending angle for the legform impactor was around 8.0°, while the bending angle for the full sized pedestrian knee exceeded 8.8°.
- The maximum shear displacement for the legform impactor was around 5.3mm, while the Shear Displacement for the full sized knee exceeded 5.9mm.
- The maximum tibia acceleration for the legform impactor was around 202g, while the Tibia Acceleration for the full sized pedestrian exceeded 217g.

Table 5.1 Overall comparison of knee bending angle

Legform Model	Model	Impact Velocity (km/h)	Knee Bending Angle[Degree]
FE Impactor	Ford Taurus	27 km/h	7.7^0
FE Impactor	Toyota Yaris	27 km/h	7.8^0
FE Impactor	Ford Taurus	40 km/h	7.9^0
FE Impactor	Toyota Yaris	40 km/h	8.0^0
Ellipsoidal Impactor	Ellipsoidal car	27 km/h	7.7
Full-size pedestrian	Ellipsoidal Car	27 km/h	8.2
Ellipsoidal Impactor	Ellipsoidal Car	40 km/h	8.0^0
Full-size pedestrian	Ellipsoidal car	40 km/h	8.8^0

5.3.2 Knee shearing displacement and tibia acceleration

The upper tibia acceleration increased as the strength of the frontal side of the car material was increased shown in Table 5.2. In all analyses, the maximum upper tibia acceleration occurred at about 5ms after collision, following an increase in acceleration. The maximum upper tibia acceleration is important for pedestrian safety. When the legform impactor was impacted by high strength material car frontal side, there was higher stiffness in the bumper beam, so upper tibia acceleration increased.

Table 5.2 Overall comparison of shear displcement and tibia acceleration

Legform Model	Model	Impact Velocity (km/h)	Shear Displacement [mm]	Tibia Acceleration [G]
FE Impactor	Ford Taurus	27 km/h	5.4	202
FE Impactor	Toyota Yaris	27 km/h	5.7	197
FE Impactor	Ford Taurus	40 km/h	5.2	201
FE Impactor	Toyota Yaris	40 km/h	5.3	202
Ellipsoidal Impactor	Ellipsoidal car	27 km/h	4.9	193
Full-size pedestrian	Ellipsoidal Car	27 km/h	5.0	210
Ellipsoidal Impactor	Ellipsoidal Car	40 km/h	5.5	198
Full-size pedestrian	Ellipsoidal car	40 km/h	5.9	217

CHAPTER 6

CONCLUSIONS AND RECOMMENDATIONS

6.1 Conclusions

This study was aimed at investigating the kinematic responses of the Finite Element legform subsystem pedestrian models and comparing them with the ellipsoidal multi body model and with the full-sized pedestrian model at different speeds. The legform-impactor vehicle collision simulations were performed using the LS-Dyna nonlinear FE coding and the MADYMO biodynamic codes, both of which are widely used to perform crash simulation simulations. At first, the models were put together and impacted according to the EEVC criteria, and the results were obtained from both simulation codes. Reasonable correlation was observed between the results from the finite element impactor model and the multibody impactor model, as well as with full-scale 50^{th} percentile full–sized pedestrian model. The injuries sustained by the pedestrian were determined from the MADYMO and LS-Dyna analyses. The most significant parameters were the knee bending angle, shear displacement and tibia risk acceleration. By developing and examining the two different approaches from the different simulation platforms, and the subsystem or full-sized pedestrian models, the appropriateness of the impactor model proposed by EEVC was demonstrated.

Same impact conditions were utilized with at velocities at 27 kmh, and 40 kmh for the simulations on different workbenches. The differences appeared in the way of the collision occurred at different speeds. In the LS-Dyna FE simulation, the impactor model was dragged towards the front-end of the car, whereas in the case of full-sized pedestrian model in MADYMO, this was not observed during the collision.

In the impact against the mid-size car model, the behavior and responses were slightly different from those from the full-sized pedestrian and impactor in the lower extremities. The kinematic responses from the impactor model were observed to be more rigid-body type response, whereas in case of the 50^{th} percentile full-sized pedestrian model, the knee bending angle was dragged or changed its nature after responding to the collision.

The affected injuries in lower leg of the pedestrian can be strongly affected by the speed and vehicle frontal side, which can be modified by reducing the stiffness properties. It was observed that bending angle for the pedestrian was above the regulation threshold criteria. When the legform impactor was impacted by high strength frontal side of car (with high stiffness in the bumper beam), deformation was quite less. This resulted in a high tibia acceleration. Impact speed has thus a significant effect on the pedestrian lower extremities when striken with a car. As speed decreases, the acceleration value also decreases. Hence, to reduce the tibia acceleration of the impactor model, the stiffness of the frontal side of car-model needs to be designed to be as soft as possible.

Observing the results from the study and comparing the pedestrian lower leg injuries on different workbenches depict the increasing number of serious implications on pedestrian impact safety. It is noted that kinematics of legform is at time noticeably different from that of the full-sized pedestrian model. Hence, despite meeting the regulation criteria, the pedestrian model exhibits slightly different response in terms of accelerations. Overall the study demonstrated that the legform impact analysis is a useful tool in predicting the potential injuries and impact responses to pedestrians. However the results from the legform impactor should be viewed with care as the actual full-sized pedestrian impact collisions might result in higher injury values and greater potential for injuries to the pedestrians.

6.2 Recommendation

The following recommendations can be made from this study for further extentsion of this research. Some recommendations are also made to avoid or to minimize pedestrian injuries by changing the car design or improving the legform impactor weights and its structure.

- The secondary impact of the pedestrian head to the car hood or ground surface needs further investigation.
- The analysis can be done with the Flex-PLI legform impactor [43] with different vehicle models.
- The FE analysis can be performed using the LS-Dyna–MADYMO coupling procedure, to better results understand the responses made by subsystem and the full-size pedestrian models. The bumper of the car model can be repositioned to more accurately examine the lower extremity injuries from the impactor.
- In terms of reducing the pedestrian injury risk, the design of the bumper can be changed, for example by using energy-absorbers materials, making the bumper edges to be smoother designs, and increasing the distance between there bonnet and engine.
- External airbags technology for the bumper and the hood can be introduced to reduce pedestrian fatalities.
- Lowering the bumper height to a suitable level can minimize risk of leg and knee injuries.
- By changing the full-size pedestrian models to different sizes, e.g., small female, large model, 6-year old child and 3-year old child models to check various kinematics responses and corresponding injury patterns are highly recommended for the study.
- Introducing automatic radar braking system using sensors on car bumper, thus detecting an object in a vehicle's path and automatically braking a car to a lower speed could be examined.

REFERENCES

REFERENCES

[1] Yang, J., "Speed Limit in City and Improvement of Vehicle Front Design for Pedestrian Impact Protection-A Computer simulation Study," Crash Safety Division, Chalmers University of Technology , Göteborg, 2000.

[2] Svoboda, J., "Pedestrian Protection-Pedestrian in Collision with Personal Car," Czech Technical University in Prague, Faculty of Mechanical Engineering, Czech Republic, 2001.

[3] Chang, D., "National Pedestrian Crash Report," U.S.Department of Transportation, Washington, DC , June 2008.

[4] "www.uwnews_org," Available: News and Information from University of Washington (uwnews), [Cited November 2016].

[5] Lefler, D.E., and Hampton, C.G., "The Fatality and Injury Risk of Light Trucks Impacts with Pedestrians in the United States," New Jersey, 2002.

[6] "Pedestrian Crash Data Study", National Transportation Sytems Center [Cited November 2016].

[7] http://www.walkinginfo.org/pdf/PedSynth/Part%202.pdf, "The Pedestrian and Bicycle Information Center." [Cited November 2016].

[8] http://www.dot.wisconsin.gov/safety/motorist/pedestrians/injuries.html.[Cited November 2016].

[9] Ishikawa, H., Kant, R., and Konosu, A, "Development of Computer Simulation Models for Pedestrian Subsystem Impact Tests," JSAE Review, 21 (2000) 109-115, 2000.

[10] Chawla, A., "Safer Truck Front Design for Pedestrian Impacts", International IRCOBI Conference on the Biomechanics of Impacts, 1998.

[11] Sherborne, D. J., Rothen J. A., and Carsten O. M. J., "Intelligent Traffic Signals for Pedestrians: Evaluation of Trials in Three Countries, Transportation Research Part C," Emerging Technologies, 1998.

[12] Sayer, J.R., and Mefford, L., "*High Visibility Safety Apparel and Nighttime Conspicuity of Pedestrians in Work Zones*," Journal of Safety Research, Vol. 35, p.537-546, 2004.

[13] May, A.J., Grimsley, P.J., and Ross, T., "*Using Traffic Light Information as Navigational Cues: Implications For Navigation System Design, Transportation Research Part F*," Traffic Psychology and Behaviour,Vol. 7,p.119-134, 2004.

[14] DeSantis Klinich K., "Techniques for developing child dummy references values," NHTSA,partly included in EEVC WG17 document 31, October 1996.

[15] Maki, T, and Asai, T., "Development of Pedestrian Protection Technologies for ASV," JSAE Review, 2002.

[16] Butera, F., Gobetto G, Ricerche C, and Zanella A., "Smart Bumper for Pedestrian Protection," Smart Materials Bulletin, , 2002.

[17] Han, Y. H.. and Lee, Y. W., "*Development of a Vehicle Structure with Enhanced Pedestrian Safety," SAE Word Congress, Detroit*, Vol.No.-01.2003.

[18] Paine M. P., and Coxon, C. G., "Assessment of Pedestrian Protection Afforded by Vehicles in Australia," Impact Biomechanics & Neck Injury, Institution of Engineers Sydney, 2000.

[19] Nasr A., Noorpoor, N., Kiasat, M.S., and Abvabi., "Lower Extremity Injuries in Vehicle-Pedestrian Collisions," Department of Automotive Engineering, Iran University of Science and Technology, Tehran, Iran, Tehran, 2009.

[20] Nguyen, T.H., and Teng, T.S., "Development and validation of FE models of impactor," Department of Mechanical and Automation Engineering, Da-Yeh University, Da-Yeh, 2008.

[21] Paulozzi, L. J., "United States pedestrian fatality rates by vehicle type," Injury Prevention, 11:232–236, Atlanta, GA, 2005.

[22] Gabler, H. C., and Hollowell, W. T., "The Aggressivity of Light Trucks and Vans in Traffic Crashes," U.S. National Highway Traffic Safety Administration, Society of Automotive Engineers., Paper No. 98-S3-O-01, 2006.

[23] Athale, N. S., "Sensitivity Analysis of Pedestrian Collision with a Small Size Family Car," M.S Thesis, Wichita State University, 2004.

[24] Ronghe, A. P., "Analysis of Pedestrian Kinematics in a Vehicle Accident," M.S. thesis, Wichita State University, 2001.

[25] Stammen, J., "Performance Of Vehicle Bumper Systems With The Eevc/Tr0L", National Highway Traffic Safety Administration , Paper No. 09-0318., 2011.

[26] Korrapati, P., "kinematic responses of the Hybrid III standing Dummy and pedestrian Human Model Kinematics in Vehicle-Pedestrian Collisions," M.S. thesis, Wichita State University, 2003.

[27] Hutchinson, J., Kaser, M.J., and Lankarani, H. M., "The Head Injury Criterion (HIC) Functional," Applied Mathematics and Computation 96 (1), 1-16, 1998.

[28] Gray, H. B., "http://www.bartleby.com -," [Cited November 2016].

[29] MADYMO Manual Realease 7.2, MADYMO, TASS, [Cited November 2016].

[30] Fontaine, H., "Typological Analysis of Pedestrian Accidents," Journée DÉtudes sur les Accidents de Piétons,, Paris, EEVC WG17., 1997.

[31] European Experimental Vechicle Committee, "Pedestrian Injury Accidents.," 9th ESV Conference, Kyoto, November 1982.

[32] European Experimental Vechicle Committee, "Cycle and Light-Powered Two-Wheeler Accidents.," 9th IRCOBI Conference, Delft, September 1984.

[33] European Experimental Vechicle Committee, "Pedestrian Injury Protection by Car Design.," 10th ESV Conference, Oxford, July 1985.

[34] Cesari, D.F., "Assessment of Test Methods to Evaluate the Protection Afforded to Pedestrians by Cars," INRETS report under Contract No.ETD/89/7750/M1/28 to the European Commission, December 1990.

[35] Brun-Cassan, F., "Assessment of Test Methods to Evaluate the Protection Afforded to Pedestrians by Cars-Compatibility," APR report under Contract No. ETD/89/7750/M1/28 to the European Commission, July 1991.

[36] Commision of the European Communities, "Frontal Surfaces In The Event of Impact With a Vulnerable Road User," Ad-hoc Working Group ERGA Passive Safety, Brussels, Document ERGA S/60., 1994.

[37] European Experimental Vechicle Committee, "Study of Test Methods to Evaluate Pedestrian Protection for Cars," EEVC Working Group 10 report, Presented to the 12th ESV Conference,, Gothenburg, 1989.

[38] Janssen, E.G., "Protection of vulnerable road users in the event of collision with a passenger car, Part I - Computer Simulations," TNO Report No. 75405002/I under Contract No. ETD/89/7750/M1/28 to the European Commission, December 1990.

[39] Janssen, E.A., "Protection of Vulnerable Road Users in the Event of Collision With a Passenger Car, Part II - Sub-systems," TNO Report No. 75405002/II under Contract No. ETD/89/7750/M1/28 to the European Commission, December 1990.

[40] Lawrence, G., "Development of a Bonnet Leading Edge Sub-systems Test to Assess Protection for Pedestrians," TRRL report under Contract No. ETD/89/7750/M1/28 to the European Commission, January 1991.

[41] Glaeser, K.P., "Development of a Head Impact Test Procedure for Pedestrian Protection.," BASt report under Contract No. ETD/89/7750/M1/28 to the European Commission, June 1991.

[42] Commision of the European Communities, "Summary of the Work of the Consortium Developing Test Methods to Evaluate the Protection Afforded to Pedestrians by cars (including test proposals," European Commission Study, July 1991.

[43] European Experimental Vechicle Committee, "Proposals for Test Methods to Evaluate Pedestrian Protection for Cars," EEVC Working Group 10 report, presented to the 13th ESV Conference, Paris, November 1991.

[44] European Experimental Vechicle Committee, "Proposals for Methods to Evaluate Pedestrian Protection for Passenger Cars.," EEVC Working Group 10 report, November 1994.

[45] European Experimental Vechicle Committee,, "EEVC test methods to evaluate pedestrian protection afforded by passenger cars," EEVC Working Group 10 report, presented to the 15th ESV Conference, Melbourne, May 1996.

[46] Stammen, J.A., Saul, R.A, and Ko, B., "Pedestrian Head Impact Testing And PCDS Recontruction," Technical Report,326., National Highway Traffic Safety Administration., 2000.

[47] Kajzer, J., and Matsui, Y., "*Shearing and Bending Effects at the Knee Joint at High Speed Lateral Loading*," SAE Paper No. 973326, EEVC WG17 Document 30, 1997.

[48] European Working Group 1 Report, "Improved Test Methods To Evaluate Pedestrian Protection Afforded By Passenger Cars," December 1998.

[49] Ishikawa, H., "A Study on Injury Criteria of EEVC Pedestrian Legform Test," JARI/JAMA,EEVC WG17 Document 85, June 1998.

[50] Schreiber, P.E.,"Static and Dynamic Bending Strength of the Leg," Proceedings IRCOBI Conference ,EEVC WG17 document 61, September 1997.

[51] Leung, Y.,"*Study of Knee-Thigh-Hip Protection Criterion,*" SAE Paper No. 831629, EEVC WG17 Document 62, 1983.

[52] Leung, Y.C., "*Study of Knee-Thigh-Hip Protection Criterion,*" SAE Paper No. 831629,EEVC WG17 document 62, 1983.

[53] National Crash Analysis Center , "www.ncac.com,"., [Cited November, 2016].

[54] www.hengstar.com, "LS-DYNA," [Cited November, 2016].

[55] LSTC, : http://www.lstc.com/products/ls-dyna, [Cited November, 2016].